Atmos. Chem. Phys., 14, 4617–4641, 2014
www.atmos-chem-phys.net/14/4617/2014/
doi:10.5194/acp-14-4617-2014

Atmospheric Chemistry and Physics Open Access

Global and regional emissions estimates for N_2O

E. Saikawa[1,2], R. G. Prinn[1], E. Dlugokencky[3], K. Ishijima[4], G. S. Dutton[3,5], B. D. Hall[3], R. Langenfelds[6], Y. Tohjima[7], T. Machida[7], M. Manizza[8], M. Rigby[9], S. O'Doherty[9], P. K. Patra[4], C. M. Harth[8], R. F. Weiss[8], P. B. Krummel[6], M. van der Schoot[6], P. J. Fraser[6], L. P. Steele[6], S. Aoki[10], T. Nakazawa[10], and J. W. Elkins[3]

[1]Center for Global Change Science, Massachusetts Institute of Technology, Cambridge, MA, USA
[2]Department of Environmental Sciences, Emory University, Atlanta, GA, USA
[3]Earth System Research Laboratory, National Oceanic and Atmospheric Administration, Boulder, CO, USA
[4]Frontier Research Center for Global Change, Yokohama, Japan
[5]Cooperative Institute for Research in Environmental Sciences, University of Colorado, Boulder, CO, USA
[6]Centre for Australian Weather and Climate Research, CSIRO Marine and Atmospheric Research, Aspendale, Victoria, Australia
[7]National Institute for Environmental Studies, Tsukuba, Japan
[8]Scripps Institution of Oceanography, University of California, San Diego, La Jolla, California, USA
[9]School of Chemistry, University of Bristol, Bristol, UK
[10]Center for Atmospheric and Oceanic Studies, Tohoku University, Sendai, Japan

Correspondence to: E. Saikawa (eri.saikawa@emory.edu)

Received: 19 June 2013 – Published in Atmos. Chem. Phys. Discuss.: 23 July 2013
Revised: 14 February 2014 – Accepted: 20 March 2014 – Published: 13 May 2014

Abstract. We present a comprehensive estimate of nitrous oxide (N_2O) emissions using observations and models from 1995 to 2008. High-frequency records of tropospheric N_2O are available from measurements at Cape Grim, Tasmania; Cape Matatula, American Samoa; Ragged Point, Barbados; Mace Head, Ireland; and at Trinidad Head, California using the Advanced Global Atmospheric Gases Experiment (AGAGE) instrumentation and calibrations. The Global Monitoring Division of the National Oceanic and Atmospheric Administration/Earth System Research Laboratory (NOAA/ESRL) has also collected discrete air samples in flasks and in situ measurements from remote sites across the globe and analyzed them for a suite of species including N_2O. In addition to these major networks, we include in situ and aircraft measurements from the National Institute of Environmental Studies (NIES) and flask measurements from the Tohoku University and Commonwealth Scientific and Industrial Research Organization (CSIRO) networks. All measurements show increasing atmospheric mole fractions of N_2O, with a varying growth rate of 0.1–0.7 % per year, resulting in a 7.4 % increase in the background atmospheric mole fraction between 1979 and 2011. Using existing emission inventories as well as bottom-up process modeling results, we first create globally gridded a priori N_2O emissions over the 37 years since 1975. We then use the three-dimensional chemical transport model, Model for Ozone and Related Chemical Tracers version 4 (MOZART v4), and a Bayesian inverse method to estimate global as well as regional annual emissions for five source sectors from 13 regions in the world. This is the first time that all of these measurements from multiple networks have been combined to determine emissions. Our inversion indicates that global and regional N_2O emissions have an increasing trend between 1995 and 2008. Despite large uncertainties, a significant increase is seen from the Asian agricultural sector in recent years, most likely due to an increase in the use of nitrogenous fertilizers, as has been suggested by previous studies.

1 Introduction

Nitrous oxide (N_2O) is a potent greenhouse gas (GHG) with a global warming potential (GWP) approximately 300 times greater than CO_2 over a 100-year time horizon (Forster et al., 2007). N_2O is also involved in stratospheric ozone depletion (Crutzen, 1970), and although its ozone-depletion potential

(ODP) is as small as 0.017, its emissions, weighted by ODP, are currently larger than those of any other ozone-depleting substances (ODSs) (Ravishankara et al., 2009). Importantly, N_2O emissions are controlled under the Kyoto Protocol, but N_2O production is not included in the Montreal Protocol on substances that deplete the ozone layer. N_2O is inert in the troposphere and is only destroyed once it reaches the stratosphere by photolysis and by chemical reaction with $O(^1D)$. Since N_2O is inert within the troposphere, it has a long atmospheric lifetime of 131 ± 10 years (Prather et al., 2012).

There are several known sources of N_2O emissions and in this paper we categorize them as the following: agricultural soil, industrial (including all combustion sources), natural soil, ocean, and biomass burning. There are large uncertainties associated with estimated emissions from each of these sectors, but approximately 2/3 of the emissions have been attributed to the natural soil and ocean, with the remaining attributed to anthropogenic sources (Khalil et al., 2002; Denman et al., 2007; Nevison et al., 2007). Included in our industrial source category are major emissions from land use change, fuel combustion for energy, and waste (European Commission, Joint Research Centre (JRC)/Netherlands Environmental Assessment Agency (PBL), 2009). The increase in atmospheric N_2O mixing ratios, since at least the 1940s, has been largely attributed to increased N_2O emissions from agricultural soils (Park et al., 2012).

Previous work has examined the source and the magnitude of these emissions with process models ("bottom-up") and with inverse methods using measurements of atmospheric mixing ratios ("top-down"). For the former, there have been efforts to quantify soil and ocean emissions. For example, Potter et al. (1996) estimated global soil N_2O emissions using an ecosystem modeling approach. Using the "hole-in-the-pipe" concept established by Firestone and Davidson (1989) and simulating with an expanded version of the Carnegie–Ames–Stanford (CASA) biosphere model (Potter et al., 1993), they estimated the global N_2O emissions from the soil to be $6.1\,TgN_2O\text{-}N\,yr^{-1}$. For global soil N_2O emissions, excluding anthropogenic nitrogen input effects, Bouwman et al. (1993) and Kreileman and Bouwman (1994) estimated emissions to be $6.6–7.0\,TgN_2O\text{-}N\,yr^{-1}$. Using the DeNitrification-DeComposition (DNDC) model developed by Li et al. (1992), Saikawa et al. (2013) estimated global natural soil N_2O emissions from 1975 to 2008 with four different available forcing data sets. Annual average estimates range from 7.4 to $11\,TgN_2O\text{-}N\,yr^{-1}$. For the ocean emissions, Nevison et al. (1995) used more than 60 000 expedition measurements to estimate global annual outgassing from the ocean to be 1.2–6.8 $TgN_2O\text{-}N\,yr^{-1}$. Recently, Manizza et al. (2012) used a large-scale ocean general circulation model coupled to a biogeochemical model to quantify the climatological mean emissions from the ocean to be $4.5\,TgN_2O\text{-}N\,yr^{-1}$.

For the top-down approach, previous work has derived global and regional N_2O emissions using the existing emissions inventories and atmospheric N_2O measurements. Prinn et al. (1990) conducted inverse modeling of N_2O at the global level using a 12-box model and quantified emissions from four latitudinal bands in the world. Hirsch et al. (2006) used a three-dimensional chemical transport model to estimate N_2O emissions from global, four semi-hemispherical and six broad regions between 1998 and 2001. Two of the results combined showed that there may have been a shift in the emissions from 30°–90° S to 0°–30° N during the period 1978–1988 to 1998–2001. Huang et al. (2008) estimated N_2O emissions during the two time periods (1997–2001 and 2002–2005), using a three-dimensional chemical transport model and estimated the global N_2O emissions to be 15.1–17.8 and $14.1–17.1\,TgN_2O\text{-}N\,yr^{-1}$ in the two periods, respectively. Kort et al. (2011) found that inversion results differ between including and excluding aircraft measurements and emphasized the importance of measurements covering the full tropospheric profile.

In this paper, drawing on insights from recent bottom-up estimates using four different forcing data sets for global natural soil emissions (Saikawa et al., 2013) and the climatological ocean emissions (Manizza et al., 2012), we first estimate approximate bottom-up monthly regional N_2O emissions by source sector on a global grid during the period 1995–2008. We use these gridded emissions as an a priori estimate for an inversion to derive regional and global emission magnitudes from the atmospheric observations. For this work, we present the new observations until the end of 2008 and use them as well as previously published N_2O atmospheric mole fraction data from several measurement networks as listed in Fig. 1 and Table 1. Although there have been papers that combined measurements from different networks for N_2O inverse modeling (e.g., Thompson et al. (2014); Corazza et al. (2011); Huang et al. (2008)), the goal of the paper was to include all available measurements (i.e., in situ, flasks, aircrafts, and ships), for the first time, from all available networks where we have reliable and consistent inter-comparison of measurements.

The paper is organized as follows: Sect. 2 describes the atmospheric measurements. Section 3 explains the inverse modeling methodology. Section 4 examines results from our inversion to analyze regional emissions by source sector. We present a summary of our results and suggestions for future research in Sect. 5.

2 Archived and ambient measurements

In this study, we use measurements of atmospheric N_2O from six networks: (1) in situ measurements from the Advanced Global Atmospheric Gases Experiment (AGAGE) network; (2) the Global Monitoring Division of NOAA's Earth System Research Laboratory (NOAA/ESRL) Carbon Cycle Greenhouse Gases (CCGG) group global cooperative air sampling flask network; (3) the NOAA/ESRL Halocarbons and other

Table 1. N_2O measurement site information.

Station	Code	Lat. (° N)	Long. (° E)	Alt.(m a.s.l.)	Data period used*	Network	Type
South Pole	SPO	−90	−24.8	2810	1/1995–12/2008	CSIRO	flask
					1/1995–12/2008	NOAA CCGG&OTTO	flask
					1/1995–12/2008	NOAA RITS&CATS	in situ
Halley Station, Antarctica	HBA	−75.6	−26.21	35.0	2/1996–12/2008	NOAA CCGG	flask
Syowa Station, Antarctica	SYO	−69.0	39.58	11.0	2/1997–12/2008	NOAA CCGG	flask
Mawson, Antarctica	MAA	−67.62	62.87	32.0	1/1995–12/2008	CSIRO	flask
Casey, Antarctica	CYA	−66.28	110.52	60.0	11/1996–12/2008	CSIRO	flask
Palmer Station, Antarctica	PSA	−64.92	−64.00		4/1997–12/2008	NOAA CCGG	flask
Drake Passage	DRP	−59	−64.69	10	4/2003–12/2008	NOAA CCGG	flask
Tierra Del Fuego, Argentina	TDF	−54.85	−68.31	32	6/1997–12/2008	NOAA CCGG	flask
Macquarie Island, Australia	MQA	−54.48	158.97	12	1/1995–12/2008	CSIRO	flask
Crozet Island, France	CRZ	−46.43	51.85	202	11/1996–12/2008	NOAA CCGG	flask
Baring Head Station, New Zealand	BHD	−41.42	174.87	95.0	10/1999–12/2008	NOAA CCGG	flask
Cape Grim, Tasmania	CGO	−40.68	144.69	21	1/1995–12/2008	CSIRO	flask
					1/1995–12/2008	AGAGE	in situ
					1/1996–12/2008	NOAA CCGG&OTTO	flask
Easter Island, Chile	EIC	−27.15	−109.45	55.0	7/1997–12/2008	NOAA CCGG	flask
Gobabeb, Namibia	NMB	−23.58	15.03	461	8/1997–12/2008	NOAA CCGG	flask
Cape Ferguson, Australia	CFA	−19.28	147.06	2.0	1/1995–12/2008	CSIRO	flask
Cape Matatula, Samoa	SMO	−14.23	−170.56	77	3/1996–12/2008	AGAGE	in situ
					1/1995–12/2008	NOAA CCGG&OTTO	flask
					1/1995–12/2008	NOAA RITS&CATS	in situ
Arembepe, Brazil	ABP	−12.76	−38.16	6.0	10/2006–12/2008	NOAA CCGG	flask
Ascension Island, UK	ASC	−7.97	−14.4	90	8/1997−-12/2008	NOAA CCGG	flask
Mahe Island, Seychelles	SEY	−4.68	55.53	3.0	6/1997–12/2008	NOAA CCGG	flask
Bukit Kototabang, Indonesia	BKT	−0.2	100.32	850.0	1/2004–12/2008	NOAA CCGG	flask
Mt. Kenya, Kenya	MKN	−0.06	37.3	3649	12/2003–12/2008	NOAA CCGG	flask
Christmas Island, Republic of Kiribati	CHR	1.70	−157.15	2.0	9/1997–12/2008	NOAA CCGG	flask
Ragged Point, Barbados	RPB	13.17	−59.43	45	6/1996–12/2008	AGAGE	in situ
					11/1995–12/2008	NOAA CCGG	flask
Mariana Islands, Guam	GMI	13.39	144.66	6.0	12/1995–12/2008	NOAA CCGG	flask
Cape Rama, India	CRI	15.08	73.83	66	1/1995–12/2008	CSIRO	flask
Cape Kumakahi, HI, USA	KUM	19.52	−154.82	3	1/1995–12/2008	NOAA CCGG&OTTO	flask
Mauna Loa, HI, USA	MLO	19.50	−155.60	3397	1/1995–12/2008	CSIRO	flask
					1/1995–12/2008	NOAA CCGG&OTTO	flask
					1/1995–12/2008	NOAA RITS&CATS	in situ
Assekrem, Algeria	ASK	23.18	5.42	1847	12/1996–12/2008	NOAA CCGG	flask
Lulin, Taiwan	LLN	23.46	120.86	2867	8/2006–12/2008	NOAA CCGG	flask
Hateruma, Japan	HAT	24.05	123.80	47	8/1996–12/2008	NIES	in situ
Key Biscayne, FL, USA	KEY	25.67	−80.20	6.0	3/1997–12/2008	NOAA CCGG	flask
Sand Island, USA	MID	28.22	−177.37	4.0	7/1997–12/2008	NOAA CCGG	flask
Tenerife, Spain	IZO	28.31	−16.48	2377.9	8/1995–12/2008	NOAA CCGG	flask
WIS Station, Israel	WIS	30.86	34.78	482	7/1997–12/2008	NOAA CCGG	flask
Moody, TX, USA	WKT	31.31	−97.33	708	2/2001–12/2008	NOAA CCGG	tower flask
Tudor Hill, Bermuda	BMW	32.26	−64.88	60.0	7/1997–12/2008	NOAA CCGG	flask
St. Davids Head, Bermuda	BME	32.37	−64.65	17.0	12/1995–12/2008	NOAA CCGG	flask
Beech Island, SC, USA	SCT	33.41	−81.83	420.0	8/2008–12/2008	NOAA CCGG	tower flask
Grifton, NC, USA	ITN	35.37	−77.39	505	3/1996–6/1999	NOAA CCGG	flask
Lampedusa, Italy	LMP	35.51	12.61	50	10/2006–12/2008	NOAA CCGG	flask
Dwejra Point, Gozo, Malta	GOZ	36.05	14.89	6.0	7/1997–2/1999	NOAA CCGG	flask
Mt. Waliguan, China	WLG	36.27	100.90	3815	4/1997–12/2008	NOAA CCGG	flask
Southern Great Plains, OK, USA	SGP	36.60	−97.48	374	4/2002–12/2008	NOAA CCGG	flask
Tae-ahn Peninsula, South Korea	TAP	36.73	126.13	21.10	7/1997–12/2008	NOAA CCGG	flask
Sutro Tower, San Francisco, CA, USA	STR	37.75	−122.45	486	10/2007–12/2008	NOAA CCGG	tower flask
Walnut Grove, CA, USA	WGC	38.26	−121.49	91	9/2007–12/2008	NOAA CCGG	tower flask
Terceira Island, Portugal	AZR	38.77	−27.38	24	10/1995–12/2008	NOAA CCGG	flask
Point Arena, CA, USA	PTA	38.95	−123.74	22.0	1/1999–12/2008	NOAA CCGG	flask
Wendover, UT, USA	UTA	39.90	−113.72	1332	12/1995–12/2008	NOAA CCGG	flask
Niwot Ridge, CO, USA	NWR	40.05	−105.58	3526	1/1995–12/2008	NOAA CCGG&OTTO	flask
					4/2002–12/2008	NOAA RITS&CATS	in situ
Boulder Atmospheric Observatory, CO, USA	BAO	40.05	−105.01	1883.96	8/2007–12/2008	NOAA CCGG	tower flask
Trinidad Head, CA, USA	THD	41.05	−124.15	107	3/1995–12/2008	AGAGE	in situ
					4/2002–12/2008	NOAA CCGG&OTTO	flask

* This is the data period used in our inversion, and some of the records extend before and after the time periods listed.

Table 1. Continued.

Station	Code	Lat. (° N)	Long. (° E)	Alt.(m a.s.l.)	Data period used*	Network	Type
Humboldt State University CA, USA	HSU	41.06	−124.75	0.0	5/2008–10/2008	NOAA CCGG	flask
Marthas Vineyard, MA, USA	MVY	41.33	−70.52	11.89	4/2007–12/2008	NOAA CCGG	flask
West Branch, IA, USA	WBI	41.72	−91.35	620.57	6/2007–12/2008	NOAA CCGG	tower flask
Cape Ochi-ishi, Japan	COI	43.16	145.50	100	6/1999–12/2008	NIES	in situ
Plateau Assy, Kazakhstan	KZM	43.25	77.88	2524	10/1997–12/2008	NOAA CCGG	flask
Black Sea, Romania	BSC	44.18	28.67	5.0	6/1997–12/2008	NOAA CCGG	flask
Sary Taukum, Kazakhstan	KZD	44.45	75.57	412	10/1997–12/2008	NOAA CCGG	flask
Ulaan Uul, Mongolia	UUM	44.45	111.10	1012	4/1997–12/2008	NOAA CCGG	flask
Argyle, ME, USA	AMT	45.03	−68.68	157.0	9/2003–12/2008	NOAA CCGG	tower flask
Cape Meares, OR, USA	CMO	45.48	−123.97	35.0	7/1997–3/1998	NOAA CCGG	flask
Park Falls, WI, USA	LEF	45.93	−90.27	868	12/1005–12/2008	NOAA CCGG	flask
Hegyhatsal, Hungary	HUN	46.95	16.65	344	11/1995–12/2008	NOAA CCGG	flask
Hohenpeissenberg, Germany	HPB	47.80	11.02	990.0	4/2006–12/2008	NOAA CCGG	flask
Estevan Point, Canada	ESP	49.38	−126.53	47.0	1/1995–12/2008	CSIRO	flask
Ochsenkopf, Germany	OXK	50.03	11.80	1185	3/2003–12/2008	NOAA CCGG	flask
Shemya Island, AK, USA	SHM	52.72	174.1	28	7/1997– 12/2008	NOAA CCGG	flask
Mace Head, Ireland	MHD	53.33	−9.90	15	1/1995–12/2008	AGAGE	in situ
					4/1999–12/2008	NOAA CCGG&OTTO	flask
Ocean Station M, Norway	STM	66.0	2.0	7.0	7/1997–12/2008	NOAA CCGG	flask
Lac La Biche, Canada	LLB	54.95	−112.45	546.1	1/2008–12/2008	NOAA CCGG	flask
Cold Bay, AK, USA	CBA	55.20	−162.72	25.0	12/1995–12/2008	NOAA CCGG	flask
Baltic Sea, Poland	BAL	55.43	16.95	28.0	6/1997–12/2008	NOAA CCGG	flask
Shetland Islands, UK	SIS	60.17	−1.17	30.0	1/1995–12 /2008	CSIRO	flask
Surgut, Russia	SUR	61	73	8 levels	1/1995–12/2008	NIES	flask
Storhofdi, Iceland	ICE	63.25	−20.15	100.0	7/1997–12/2008	NOAA CCGG	flask
Pallas-Sammaltunturi, Finland	PAL	67.97	24.12	565	12/2001–12/2008	NOAA CCGG	flask
Pt. Barrow, AK, USA	BRW	71.30	−156.60	11	1/1995–12/2008	NOAA CCGG&OTTO	flask
					1/1995–12/2008	NOAA RITS&CATS	in situ
Summit, Greenland	SUM	72.60	−38.40	3214.54	6/1997–12/2008	NOAA CCGG&OTTO	flask
					6/1997–12/2008	NOAA CATS	in situ
Mould Bay, Canada	MBC	76.25	−119.35	35.0	1/1997–5/1997	NOAA CCGG	flask
Ny-Ålesund, Norway	ZEP	78.91	11.88	479	3/1997–12/2008	NOAA CCGG	flask
Alert, Canada	ALT	82.45	−62.52	205	1/1995–12/2008	CSIRO	flask
					11/1995–12/2008	NOAA CCGG&OTTO	flask
South China Sea (3° N)	SCSN03	3.00	105.00	20.0	7/1997–10/1998	NOAA CCGG	flask
South China Sea (6° N)	SCSN06	6.00	107.00	20.0	7/1997–10/1998	NOAA CCGG	flask
South China Sea (9° N)	SCSN09	9.00	105.00	20.0	7/1997–10/1998	NOAA CCGG	flask
South China Sea (12° N)	SCSN12	12.00	105.00	20.0	7/1997–10/1998	NOAA CCGG	flask
South China Sea (15° N)	SCSN15	15.00	105.00	20.0	7/1997–10/1998	NOAA CCGG	flask
South China Sea (18° N)	SCSN18	18.00	105.00	20.0	7/1997–10/1998	NOAA CCGG	flask
South China Sea (21° N)	SCSN21	21.00	105.00	20.0	7/1997–10/1998	NOAA CCGG	flask
Pacific Ocean (0° N)	POC000	0.00	−155.00	20.00	12/1995–12/2008	NOAA CCGG&Tohoku	flask
Pacific Ocean (5° N)	POCN05	5.00	−151.00	20.00	12/1995–12/2008	NOAA CCGG&Tohoku	flask
Pacific Ocean (10° N)	POCN10	10.00	−149.00	20.00	12/1995–12/2008	NOAA CCGG&Tohoku	flask
Pacific Ocean (15° N)	POCN15	15.00	−145.00	20.00	12/1995–12/2008	NOAA CCGG&Tohoku	flask
Pacific Ocean (20° N)	POCN20	20.00	−141.00	20.00	12/1995–12/2008	NOAA CCGG&Tohoku	flask
Pacific Ocean (25° N)	POCN25	25.00	−139.00	20.00	12/1995–12/2008	NOAA CCGG&Tohoku	flask
Pacific Ocean (30° N)	POCN30	30.00	−135.00	20.00	12/1995–12/2008	NOAA CCGG&Tohoku	flask
Pacific Ocean (5° S)	POCS05	−5.00	−159.00	20.00	12/1995–12/2008	NOAA CCGG&Tohoku	flask
Pacific Ocean (10° S)	POCS10	−10.00	−161.00	20.00	12/1995–12/2008	NOAA CCGG&Tohoku	flask
Pacific Ocean (15° S)	POCS15	−15.00	−172.00	20.00	12/1995–12/2008	NOAA CCGG&Tohoku	flask
Pacific Ocean (20° S)	POCS20	−20.00	−174.00	20.00	12/1995–12/2008	NOAA CCGG&Tohoku	flask
Pacific Ocean (25° S)	POCS25	−25.00	−171.00	20.00	12/1995–12/2008	NOAA CCGG&Tohoku	flask
Pacific Ocean (30° S)	POCS30	−30.00	−176.00	20.00	12/1995–12/2008	NOAA CCGG&Tohoku	flask
Pacific Ocean (35° S)	POCS35	−35.00	180.00	20.00	12/1995–12/2008	NOAA CCGG&Tohoku	flask
Western Pacific Cruise	WPC	−30–35	136–170.5	8.0	5/2004–9/2008	NOAA CCGG	flask

* This is the data period used in our inversion, and some of the records extend before and after the time periods listed.

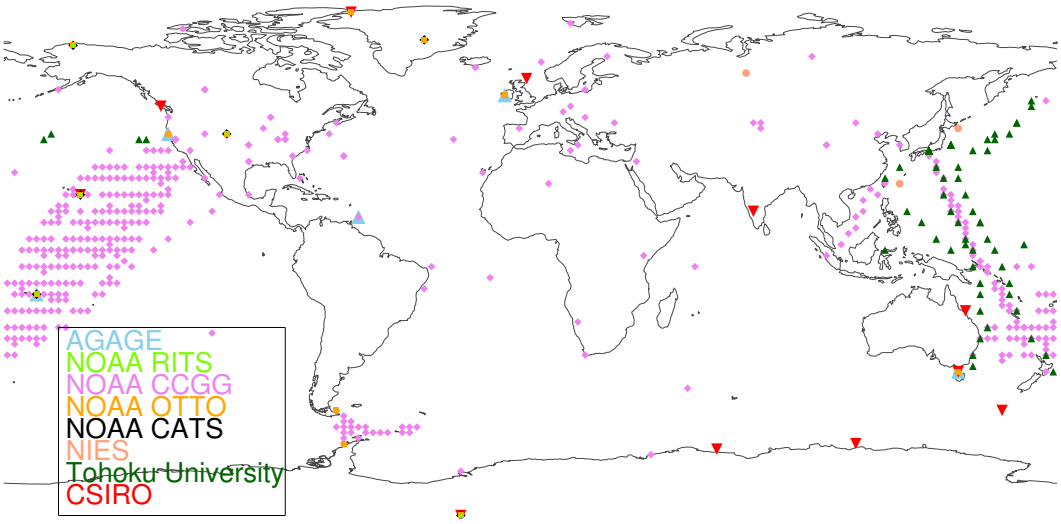

Fig. 1. Sampling networks and locations for the measurements used in the N_2O inversions. See also Table 1.

Atmospheric Trace Species (HATS) discrete sample (flask) (OTTO) and in situ (Radiatively Important Trace Species, RITS and Chromatograph for Atmospheric Trace Species, CATS) network; (4) the Commonwealth Scientific and Industrial Research Organization (CSIRO) flask sampling network; (5) the National Institute for Environmental Studies (NIES) in situ and Surgut aircraft measurement network, and (6) the Tohoku University flask measurement network. We use them for our inversions to estimate the emissions of N_2O. Within the AGAGE network, high-frequency in situ measurements of N_2O have been carried out using gas chromatography with electron capture detection (GC/ECD) (Prinn et al., 2000) at five sites since 1978. In this study, we use measurements of the air sampled at the following AGAGE sites: Cape Grim, Tasmania; Trinidad Head, California, USA; Mace Head, Ireland; Ragged Point, Barbados; and Cape Matatula, American Samoa (see Fig. 1 and Table 1). Stations that previously existed at Cape Meares, Oregon (1979–1989) and at Adrigole, Ireland (1978–1983) were replaced by Trinidad Head and Mace Head, respectively. All AGAGE in situ measurements are calibrated using the SIO-98 absolute calibration scale. The estimate of all the errors involved in the calibration scale such as reagent purity, possible analytical interferences, statistics of primary standard preparation, and propagation is approximately 0.5 %.

At NOAA/ESRL, discrete air samples have been collected at remote locations and analyzed for N_2O since 1997 as part of the CCGG global cooperative air sampling network (Dlugokencky et al., 1994). Samples of air are collected regularly in paired glass flasks (2–3 L) and pressurized to 0.20 MPa, and analyzed on one of two GC/ECD instruments in Boulder, Colorado. In this study, we use measurements from 72 sites (Fig. 1 and Table 1). Repeatability of the analytical system is 0.2 ppb (1σ), and the total uncertainty including reagent purity, interferences, etc. is 1.0 ppb (0.3 %).

In situ and flask measurements are also collected by the NOAA HATS program over the globe. The NOAA RITS in situ program started at the following four stations in 1987: Barrow, AK, USA; Mauna Loa, HI, USA; Cape Matatula, American Samoa; and South Pole, as well as in Niwot Ridge, CO, USA in 1990. The CATS program started using new in situ gas chromatographs at all of the above-mentioned five sites, and also added Summit, Greenland in 2007. The OTTO program has also collected flasks at weekly to monthly intervals from the above six stations as well as at the seven following sites: Alert, Canada; Cape Kumukahi, HI, USA; Cape Grim, Australia; Palmer Station, Antarctica; Mace Head, Ireland; Trinidad Head, CA, USA; and Tierra del Fuego, Argentina. All NOAA measurements are on the NOAA-2006A N_2O scale (Hall et al., 2007), and the estimate of all the errors for the OTTO, RITS, and CATS programs is less than 0.4 ppb (0.1 %) (Hall et al., 2007).

We also use flask measurements from the CSIRO network (Francey et al., 1996, 2003). There are 11 measurement sites including the one at Cape Rama, India (Fig. 1 and Table 1). The flasks have been collected at weekly to monthly intervals at these sites and are analyzed by GC/ECD at CSIRO. The measurements are referenced to the NOAA-2006A N_2O scale (Hall et al., 2007). Repeatability of the analytical system is 0.3 ppb (1σ), and the estimate of the error in accuracy is less than 0.1 % for the majority of the samples.

NIES has been measuring N_2O at two field sites (Hateruma Island and Cape Ochiishi, see Fig. 1 and Table 1). These N_2O measurements are calibrated using the NIES-96 scale (Tohjima et al., 2000). The precision of the measurement system is approximately 0.3 ppb ($1\,\sigma$) and the estimate of the error in accuracy is approximately 0.4 ppb (0.1 %).

Monthly aircraft measurements have been made near the city of Surgut, Russia since July 1993, using a chartered aircraft as described in Ishijima et al. (2010). Outside air

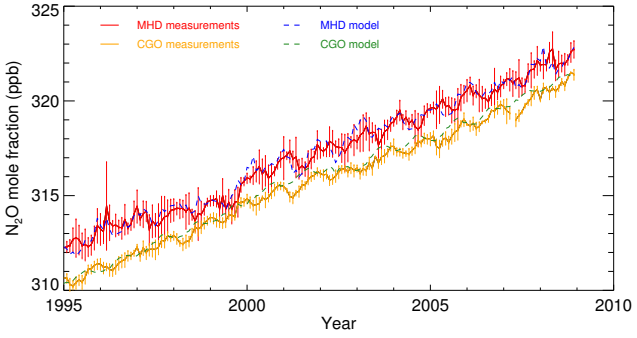

Fig. 2. Combined N_2O observations at Cape Grim, Tasmania (CGO, orange) and Mace Head, Ireland (MHD, red) from AGAGE and NOAA networks. Atmospheric mole fractions predicted by MOZART v4 using optimized emissions with GMFD prior emissions estimates for natural soil are shown in dashed lines for CGO (green) and MHD (blue).

is collected at 0.5, 1, 1.5, 2, 3, 4, 5.5, and 7 km above the surface in glass flasks, pressurized and then analyzed by an GC/ECD instrument in NIES. The NIES-96 N_2O scale is used for calibration, and the repeatability of the analytical system is 0.3 ppb. The estimate of the error in accuracy is approximately 0.4 ppb (0.1 %).

The Tohoku University group has been measuring N_2O at multiple locations using aircraft and ships since 1991 (Ishijima et al., 2001, 2009, 2010). Collected air samples are analyzed using the GC/ECD at Tohoku University. The data between 2003 and 2009 are new and cover a wide latitude range from the north of Japan to the Oceania region (see Fig. 1). These N_2O measurements are calibrated using the Tohoku University scale. Repeatability of the flask samples is 1.0 ppb until 2001 and 0.3 ppb since 2002, and the estimate of the error in accuracy is approximately 0.2 %.

We compare atmospheric N_2O measurements collected from each group, as they are based on different absolute calibration scales (Table 2) and differences exist among measurement networks. Because the global average mole fraction of N_2O increases at approximately 0.2–0.3 % per year (see Fig. 2), the calibration ratio of 0.9975 corresponds to a one year's rise in mole fraction, and thus a calibration difference as small as 0.6 % can be significant. Hence, it is very important for us to adjust all of the measurements into a single scale referenced to that of AGAGE, even though calibration scales appear to be close to one another. Shifts in the differences between co-located measurements result from uncertainty in propagating the scale to in situ measurement sites, and those shifts result from various factors, but the standard calibration scales do not change over time. We include generous uncertainties to account for these shifts in the differences over time, and this divergence is small compared to other uncertainties.

First, the comparisons between AGAGE and NOAA are conducted using measurements collected at the same site at approximately the same time. NOAA CCGG flask samples collected at the four AGAGE sites (CGO, SMO, RPB, and MHD) between 1997 and 2012 and at THD between 2002 and 2012 were compared with AGAGE GC-ECD in situ measurements at those sites. Data from the two networks agree well in general for N_2O with a mean ratio (CCGG/AGAGE) of 0.9994 and a standard deviation of 0.0005 for the matching mixing ratios. In addition, NOAA CATS in situ samples collected at SMO from 2000 to 2012 were compared with AGAGE GC-ECD in situ measurements at the same site. The data also agree well with a mean ratio (CATS/AGAGE) of 1.0009 and a standard deviation of 0.0010. RITS measurements compare well with CATS, and thus we use the same factor for both. We therefore adjust the NOAA measurements to the SIO-98 scale by applying 1.0006 for CCGG flask and 0.9991 for OTTO, RITS, and CATS in our inversions. We also apply an offset factor for the measurements taken in the OTTO network as a difference from the CATS measurements at the same site. The adjustment is 1.3 ppb at American Samoa and 0.6 ppb elsewhere.

Second, the comparisons between the AGAGE and CSIRO networks are conducted at the CGO site, where the average difference is 0.35 ppb (AGAGE-CSIRO), which is equivalent to the ratio (CSIRO/AGAGE) of 0.9989. Therefore, we adjust the CSIRO flask network measurements by applying a factor of 1.0011 in our inversions.

Third, the comparisons between NOAA CATS and Tohoku University, as well as between NIES and Tohoku University, are conducted at the same site at approximately the same time. On average, Tohoku University measurements are 0.2 ppb and 0.8 ppb higher than NOAA and NIES measurements, respectively. These values translate into the mean ratios (Tohoku/CATS and Tohoku/NIES) of about 1.0006 and 1.0025. These two comparisons also allow us to quantify the constant offset values between CATS and NIES measurements (CATS-NIES) of 0.6 ppb with a ratio (CATS/NIES) of approximately 1.0019. Based on these comparisons, the ratios (Tohoku/AGAGE and NIES/AGAGE) are approximately 1.0015 and 0.9990. Therefore, we apply 0.9985 and 1.0011 to convert Tohoku and NIES measurements into the SIO-98 scale.

3 Emissions inversion method

Using reasonable prior estimates of annual regional N_2O emissions by source sector and the three-dimensional chemical transport model, Model for Ozone and Related Chemical Tracers version 4 (MOZART v4), we apply an inverse method to estimate annual regional emissions by source sector using the measurements of N_2O atmospheric mole fractions discussed above. In this section, we outline our inverse modeling methodology.

Table 2. Calibration information among the six measurement networks.

Network	Calibration ratio to AGAGE	Measurement error	Scale propagation error
AGAGE	1	0.1 %	0.012 %
NOAA CCGG	0.9994	0.1 %	0.07 %
NOAA OTTO&RITS&CATS	1.0009*	0.2 %	0.07 %
NIES	0.9990	0.1 %	0.03 %
CSIRO	0.9989	0.1 %	0.016 %
Tohoku University	1.001	0.3 % before 2002 and 0.1 % since 2002	0.03 %

* Offset values are applied to NOAA OTTO network measurements (1.3 ppb at SMO and 0.6 ppb elsewhere).

3.1 Prior emission estimates

For conducting inversions, we created a priori emission estimates by combining the existing emissions inventory for the three sectors (i.e., industrial, agricultural soil, and biomass burning) with new estimates from two process models for the ocean and natural soil. For industrial and agricultural soil emissions, we used the EDGAR v4.1 emissions with a spatial resolution of 1° latitude × 1° longitude (European Commission, Joint Research Centre (JRC)/Netherlands Environmental Assessment Agency (PBL), 2009). EDGAR provides gridded emissions every 5 years between 1970 and 2000, and annually between 2000 and 2005. We therefore interpolated annual emissions based on the growth rate to fill gaps and extrapolated to 2008 by taking the average annual growth rate between 2001 and 2005. For biomass burning emissions, we used the Global Fire Emissions Database version 3 (GFED v3) with a spatial resolution of 0.5° latitude × 0.5° longitude (van der Werf et al., 2010). GFED v3 provides monthly emissions between 1997 and 2008, so we extrapolated for years between 1990 and 1996 by applying the average annual growth rate between 1997 and 2008.

Manizza et al. (2012) estimated climatological monthly air–sea N_2O fluxes using a bottom-up process modeling approach. Their model includes both denitrification and nitrification process-induced fluxes at a spatial resolution of 2.8° latitude × 2.8° longitude. They adopted the parameterization of Suntharalingam and Sarmiento (2000) for the production of N_2O in the water column. A more detailed description of their physical and biogeochemical model can be found in Manizza et al. (2012).

For natural soil emissions, we use another newly developed process model (CLMCN-N_2O) that is able to reproduce the seasonality and inter-annual variability of global emissions at some sites (e.g., Amazon) but not at others (e.g., North America) (Saikawa et al., 2013). This model is an addition to the Community Land Model with coupled Carbon and Nitrogen cycles version 3.5 (CLM-CN v3.5) (Thornton et al., 2007; Thornton et al., 2009; Randerson et al., 2009). CLMCN-N_2O includes the DeNitrification-DeComposition (DNDC) Biogeochemistry Model (Li et al., 1992), and similarly to the ocean process model, it captures both the nitrification and denitrification processes that are important producers of N_2O in soil. The four forcing data sets used are Global Meteorological Forcing Dataset (GMFD) by Sheffield et al. (2006); NCEP Corrected by CRU (NCC) by Ngo-Duc et al. (2005); Climate Analysis Section (CAS) by Qian et al. (2006); and Global Offline Land-Surface Dataset (GOLD) by Dirmeyer and Tan (2001) and Betts et al. (2006).

For our regional inversion, we assume 40 % uncertainty for our prior values for the emissions from all sources, sectors, and regions. This range, decided empirically based on previous studies (i.e., Hirsch et al. (2006); Huang et al. (2008)), is justifiable as there have been high uncertainties in N_2O emissions, especially in recent years after an increased agricultural nitrogen fertilizer use in developing countries. We also note that although we separate the emissions from different sectors, in reality nitrogen fertilizer applied to agricultural soil, for example, can be leached into rivers and thus on to the ocean, where it can be emitted as N_2O. But the effect of these transfers on emissions have significant uncertainty in existing inventories and process models so the aim of our inversions is to improve the existing emissions inventories and the process model results using atmospheric observations.

3.2 Global chemical transport model

The global three-dimensional chemical transport model, MOZART v4 (Emmons et al., 2010) is used to simulate the three-dimensional N_2O atmospheric mole fractions between 1995 and 2008. MOZART v4 is a model for the troposphere, has updates over the previous MOZART version 2, and is built on the framework of the Model of Atmospheric Transport and Chemistry (MATCH) (Rasch et al., 1997). Previous studies have found too strong net downward transport from the stratosphere in the model using the reanalysis meteorology (Holloway et al., 2000; van Noije et al., 2004; Xiao et al., 2010) resulting, for example, in errors in the tropospheric ozone budget as well as in the ozone mixing ratios in the upper troposphere (Emmons et al., 2010). Because this can lead to a potentially large bias in our analysis, we restricted ourselves to estimating regional annual and not monthly emissions by source sector. This, however, provides new annual estimates for 14 years at the regional level and by the source sector globally, which is an advancement from

past studies (i.e., Hirsch et al. (2006); Huang et al. (2008); Thompson et al. (2011); Corazza et al. (2011)). The horizontal resolution of MOZART v4 is 1.9° latitude × 2.5° longitude, including 56 vertical levels from the surface to approximately 2 hPa. Chemical and transport processes are driven by the annually varying Modern Era Retrospective-analysis for Research and Applications (MERRA) meteorological fields (Rienecker et al., 2011).

We assume that N_2O is inert in the troposphere and chemical loss is by photolysis and reaction with $O(^1D)$ in the stratosphere. The spatial and temporal pattern of the inter-annually changing photolysis field is calculated for the three wavelength-ranges 200–217 nm, 217–230 nm and 230–278 nm, and it includes the temperature dependency of the absorption cross sections, similarly to Ishijima et al. (2010). For the wavelength band 178–200 nm, Minschwaner et al. (1993) is used. The annually repeating $O(^1D)$ field is estimated using the LMDZ4-INCA2 global climate model (Hourdin et al., 2006). Both of these fields are interpolated to match our horizontal and vertical resolutions, conserving the mass. The spinup was done for 10 years starting with a uniform latitudinal mixing ratio and with vertical distributions based on observations. We then compared surface mixing ratios to available observations in 1995 to start the simulation. The lifetime of N_2O, calculated by the ratio of the annual total global burden to the loss rate calculated in the chemical transport model is 116 ± 5 yr, which is slightly lower than the current estimate of 131 ± 10 yr by Prather et al. (2012) but is in alignment of 114 years with Montzka et al. (2011).

We estimate emissions from seven land regions and six ocean regions for 5 source sectors between 1995 and 2008 incorporating all the measurements in Table 1, including all data without pollution event filtering. The MERRA meteorological reanalyses were used at 6-hourly intervals, and the model was run with a 15-minute time step. When there were measurements from multiple different networks, we first generated monthly averages for each network at each site, and then combined the data sets to create monthly averages and standard deviations at a site using the number of measurement-weighted averages, accounting for the different measurement frequency (e.g., flask versus in situ sampling) at each station in the various networks.

3.3 Sensitivity estimates and inverse method

To conduct inverse modeling, we follow the methodology in Saikawa et al. (2012). We quantify the atmospheric mole fractions response to an increase in emissions for each sector and region at each measurement site (which we herein call the "sensitivity") using the global chemical transport model MOZART v4. We incorporate these sensitivity values into a matrix **H** and estimate emissions by deriving a Bayesian weighted least-squares solution. This technique provides an optimal estimate by minimizing the following cost function with respect to x:

$$J = (y - \mathbf{H}x)^T \mathbf{W}^{-1} (y - \mathbf{H}x) + x^T \mathbf{S}^{-1} x, \quad (1)$$

where y is the vector of the difference between measurements and modeled mole fractions, x is the vector of the difference between the prior and the optimized emissions, **W** is the measurement uncertainty covariance matrix, and **S** is the prior uncertainty covariance matrix. **W** and **S** are both diagonal matrices.

3.4 Measurement-model uncertainty estimation

Five types of uncertainty were considered for total measurement uncertainty: errors in the measurements themselves (precision), scale propagation error, sampling frequency error, model-data mismatch (representation) error, and model transport and aggregation error. The total variance is therefore calculated by combining the five types as follows, assuming that they are uncorrelated (e.g., Chen and Prinn (2006) and Rigby et al. (2010)):

$$\sigma^2 = \sigma^2_{\text{measurement}} + \sigma^2_{\text{scale propagation}} + \sigma^2_{\text{sampling frequency}} + \sigma^2_{\text{mismatch}} + \sigma^2_{\text{model}}. \quad (2)$$

Here the measurement error $\sigma_{\text{measurement}}$ is the estimated total uncertainty due to the repeatability of each measurement (precision) at each site. The instrumental precision of N_2O is approximately 0.1 % for AGAGE, NOAA CCGG, NIES, and CSIRO, 0.2 % for NOAA OTTO, RITS, and CATS, and 0.3 % before 2002 and 0.1 % since 2002 for Tohoku University, and thus these values are included as our instrumental precision errors in this study. The error $\sigma_{\text{scale propagation}}$ arises in the chain that links the primary standards to ambient air measurements. For N_2O, the mean assumed scale propagation error was approximately 0.006–0.012 % for all the SIO, 0.07 % for NOAA CCGG and OTTO, RITS, and CATS, 0.016 % for CSIRO, and 0.015–0.03 % for NIES and Tohoku University scales, respectively. We therefore include 0.012 %, 0.07 %, 0.016 %, and 0.03 % for all the data that come from AGAGE, for NOAA, for CSIRO, and for NIES and Tohoku University, respectively.

The error $\sigma_{\text{sampling frequency}}$ accounts for the number of samples measured in a month to create a monthly mean for each measurement site (Chen and Prinn, 2006). Because of the difference in the number of measurements in a month between high-frequency observations (every 2 h) and weekly flask measurements, this error is approximately 3 to 10 times lower for high-frequency observations, compared with the error associated with NOAA and AGAGE measurements at the same site. Even when we assume a 10-hour serial correlation for the AGAGE in situ measurements (resulting in approximately 70 uncorrelated measurements in a month), it does not affect the results in any substantial way (the largest difference being less than 0.5 % change in optimized emissions).

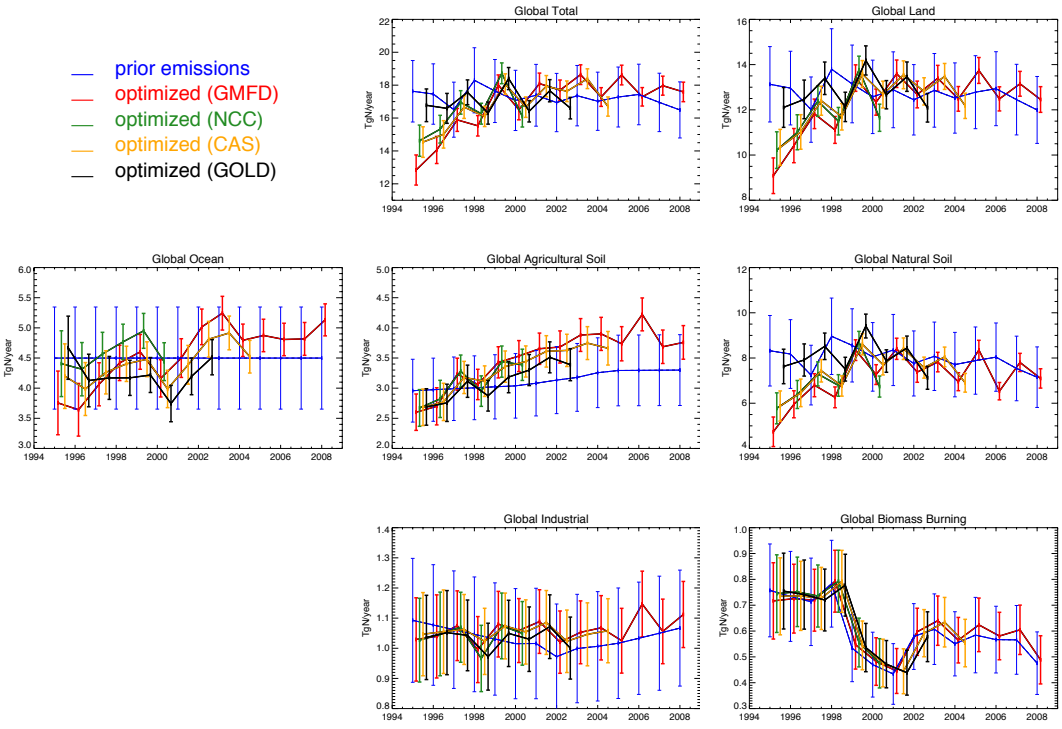

Fig. 3a. Comparison of prior (blue) and optimized global total, global land, and global emissions from each sector (ocean, agricultural soil, natural soil, industrial, and biomass burning) in $TgN_2O\text{-}N\ yr^{-1}$ from four inversions, each using a different forcing data set for natural soil (red: GMFD; green: NCC; orange: CAS; and blue: GOLD). Prior emissions shown are those with natural soil emissions using GMFD forcing data uncertainties and prior emissions are 40 %, whereas posterior uncertainties are one standard deviation.

The error σ_{mismatch} describes the difference between a point measurement and a model-simulated observation that represents a large volume of air (Prinn, 2000; Chen and Prinn, 2006). As in Saikawa et al. (2012), we calculate it from the following equation:

$$\sigma_{\text{mismatch}} = \sqrt{\frac{1}{8}\sum_{i=1}^{8}(y_i - y)^2}, \quad (3)$$

where y_i is the atmospheric mole fraction in a grid box surrounding the measurement site location i, and y is the mole fraction in the grid cell at the measurement site. Similarly to the sampling frequency error, the mismatch error also varies by month at each site, taking into account the monthly changes in transport in the model.

Finally, σ_{model} is the error associated with the global chemical transport model, which we choose to interpret as an additional measurement error. One contribution to this error is transport error that in the model inter-comparison study of Thompson et al. (2014) implies that there is approximately a 0.2 ppb difference among various chemical transport models, which translates into 0.06 % uncertainty. A significant "aggregation" error is also possible when solving for aggregated regions as we do here, because we assume that the spatial distribution in the prior emissions is correct (e.g., Kaminski et al. (2001); Engelen et al. (2002); Meirink et al. (2008)). This "aggregation" error is also incorporated in our model error, with a value of 0.8 % in our inversion, as Kaminski et al. (2001) find the highest aggregation error of 3 ppm out of 370 ppm in CO_2 in summer at Cape Grim, Tasmania. Summing the two errors in quadrature gives a total model error of 0.8 %.

4 Results and discussions

4.1 Regional emissions by source sector between 1995 and 2008

In this section, we present results from our inversion to derive regional N_2O emissions by source sector for the 13 regions using all available data from AGAGE, NOAA CCGG, NOAA OTTO, RITS, and CATS, CSIRO, NIES, and Tohoku University networks (Fig. 1 and Table 1), as well as MOZART v4. We seek to determine the locations and magnitudes of these emissions, and if we see any change in the recent years from a specific region or sector.

We created the regions based on their proximity to the measurement sites, and with the intention of separating emissions based on large ocean groups. For those areas very distant from these sites the regions are entire continents, and if there are sufficient measurements, we divided the continent

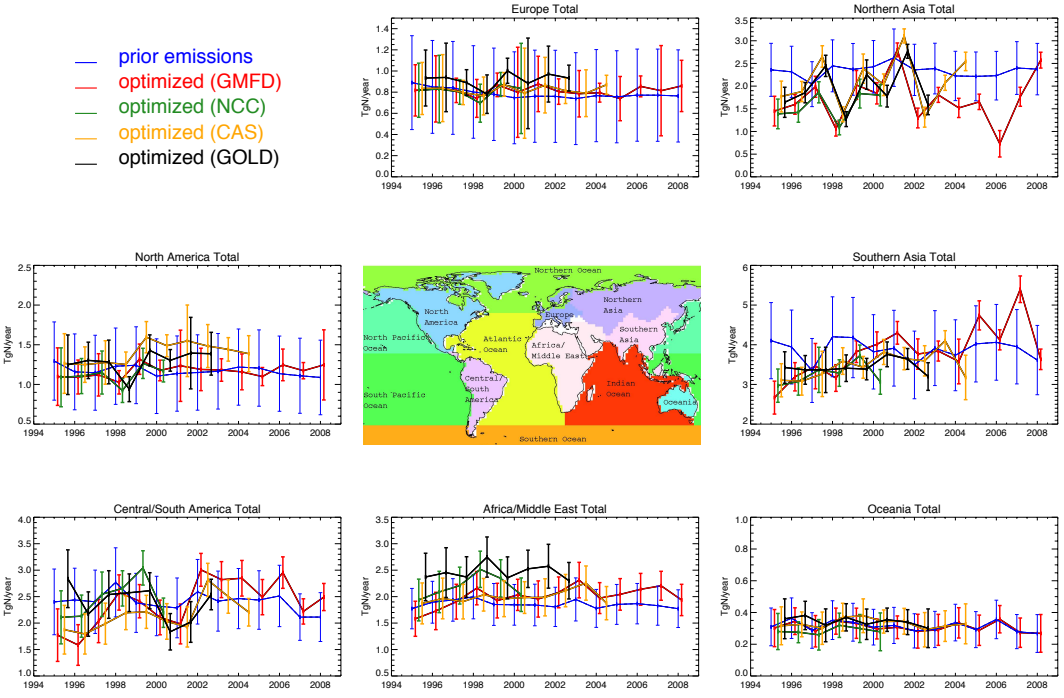

Fig. 3b. Comparison of prior (blue) and optimized emissions from each region (Europe, Northern Asia, North America, Southern Asia, Central/South America, Africa/Middle East, and Oceania) in $TgN_2O\text{-}N\,yr^{-1}$ from four inversions for seven regions, each using a different forcing data set for natural soil (red: GMFD; green: NCC; orange: CAS; and black: GOLD). Prior emissions shown are those with natural soil emissions using GMFD forcing data and prior emissions uncertainties are 40 %, whereas posterior uncertainties are one standard deviation.

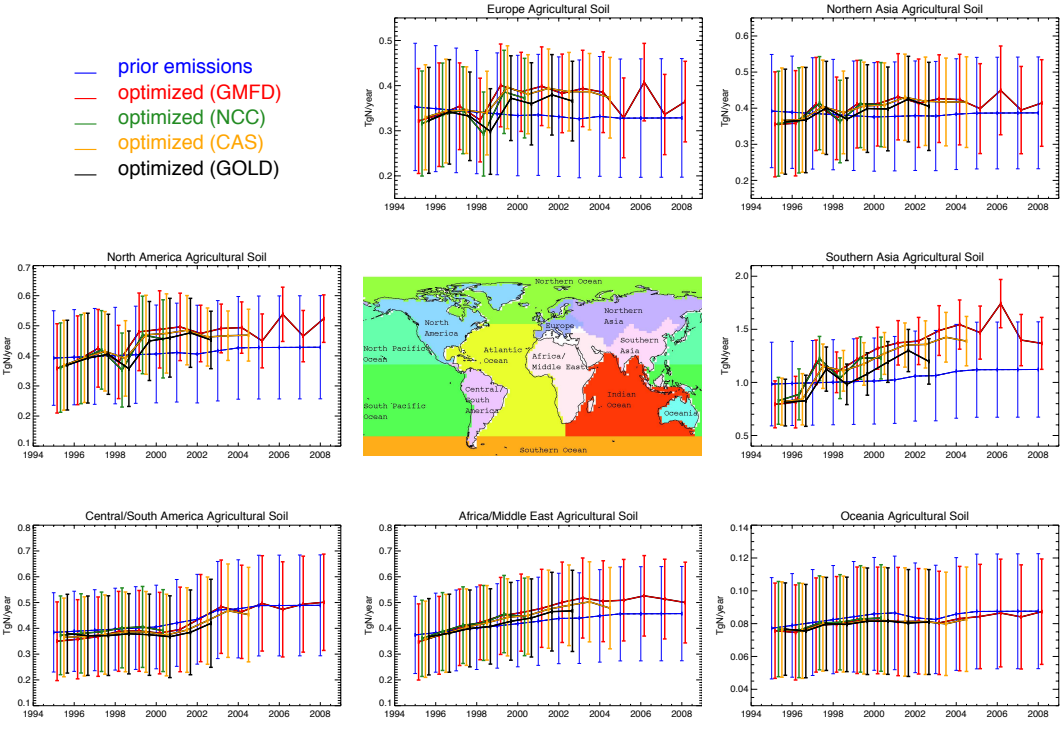

Fig. 3c. Comparison of prior (blue) and optimized agricultural soil emissions in $TgN_2O\text{-}N\,yr^{-1}$ from four inversions for seven regions, each using a different forcing data set for natural soil (red: GMFD; green: NCC; orange: CAS; and black: GOLD). Prior emissions uncertainties are 40 %, and posterior uncertainties are one standard deviation.

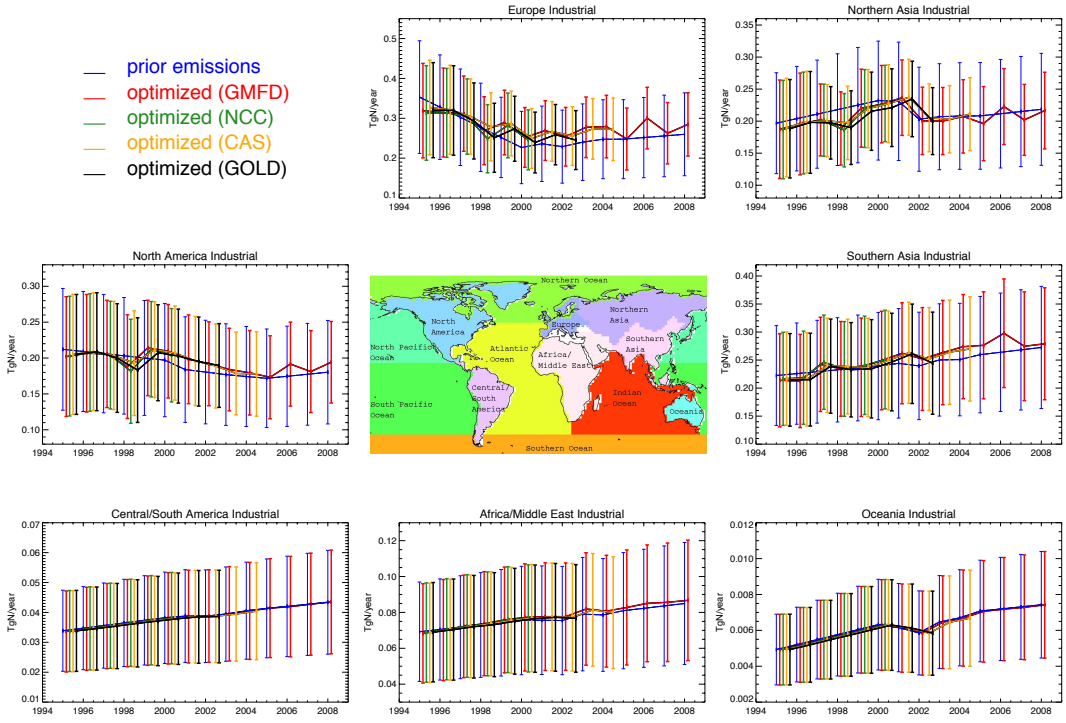

Fig. 3d. Comparison of prior (blue) and optimized industrial emissions in $TgN_2O\text{-}N\ yr^{-1}$ from four inversions for seven regions, each using a different forcing data set for natural soil (red: GMFD; green: NCC; orange: CAS; and black: GOLD). Prior emissions uncertainties are 40 %, and posterior uncertainties are one standard deviation.

Table 3. Prior and optimized global, global land, ocean, and total N_2O emissions by source sector with uncertainties using the GMFD forcing data sets for natural soil ($TgN_2O\text{-}N\ yr^{-1}$).

	Global total		Global land		Ocean		Agricultural soil		Natural soil		Industrial		Biomass burning	
Year	Prior	Posterior	Prior	Posterior	Prior	Posterior	Prior	Posterior	Prior	Posterior	Prior	Posterior	Prior	Posterior
1995	17.63	12.84	13.13	9.08	4.50	3.76	2.96	2.60	8.32	4.74	1.09	1.03	0.76	0.72
	(±1.87)	(±0.92)	(±1.67)	(±0.79)	(±0.85)	(±0.53)	(±0.52)	(±0.30)	(±1.56)	(±0.65)	(±0.21)	(±0.14)	(±0.18)	(±0.15)
1996	17.46	14.06	12.96	10.42	4.50	3.64	2.97	2.70	8.18	5.95	1.08	1.04	0.73	0.73
	(±1.84)	(±0.82)	(±1.63)	(±0.76)	(±0.85)	(±0.44)	(±0.52)	(±0.31)	(±1.52)	(±0.60)	(±0.20)	(±0.14)	(±0.17)	(±0.13)
1997	16.51	15.89	12.01	11.82	4.50	4.06	2.99	3.23	7.24	6.80	1.06	1.07	0.71	0.72
	(±1.67)	(±0.70)	(±1.44)	(±0.65)	(±0.85)	(±0.36)	(±0.53)	(±0.27)	(±1.32)	(±0.51)	(±0.19)	(±0.12)	(±0.17)	(±0.12)
1998	18.30	15.53	13.80	11.11	4.50	4.42	3.01	3.06	8.96	6.26	1.05	1.00	0.78	0.79
	(±1.98)	(±0.62)	(±1.79)	(±0.59)	(±0.85)	(±0.29)	(±0.53)	(±0.25)	(±1.69)	(±0.46)	(±0.19)	(±0.11)	(±0.17)	(±0.12)
1999	17.64	18.01	13.14	13.40	4.50	4.60	3.02	3.43	8.56	8.35	1.03	1.08	0.53	0.55
	(±1.92)	(±0.62)	(±1.72)	(±0.59)	(±0.85)	(±0.29)	(±0.53)	(±0.26)	(±1.62)	(±0.46)	(±0.19)	(±0.11)	(±0.13)	(±0.09)
2000	17.07	16.50	12.57	12.34	4.50	4.16	3.04	3.53	8.05	7.27	1.02	1.06	0.47	0.48
	(±1.83)	(±0.61)	(±1.62)	(±0.58)	(±0.85)	(±0.31)	(±0.54)	(±0.26)	(±1.52)	(±0.44)	(±0.18)	(±0.11)	(±0.13)	(±0.09)
2001	17.38	18.09	12.89	13.60	4.50	4.50	3.08	3.65	8.35	8.41	1.02	1.09	0.43	0.45
	(±1.88)	(±0.64)	(±1.68)	(±0.61)	(±0.85)	(±0.32)	(±0.54)	(±0.26)	(±1.57)	(±0.47)	(±0.18)	(±0.11)	(±0.12)	(±0.09)
2002	16.94	17.69	12.44	12.68	4.50	5.02	3.13	3.68	7.76	7.38	0.97	1.02	0.58	0.60
	(±1.77)	(±0.62)	(±1.56)	(±0.59)	(±0.85)	(±0.30)	(±0.56)	(±0.27)	(±1.44)	(±0.45)	(±0.17)	(±0.10)	(±0.13)	(±0.09)
2003	17.36	18.64	12.86	13.39	4.50	5.24	3.18	3.88	8.08	7.82	1.00	1.05	0.61	0.64
	(±1.84)	(±0.60)	(±1.63)	(±0.57)	(±0.85)	(±0.28)	(±0.56)	(±0.27)	(±1.51)	(±0.43)	(±0.18)	(±0.10)	(±0.14)	(±0.10)
2004	17.02	17.28	12.52	12.48	4.50	4.79	3.26	3.90	7.71	6.95	1.01	1.07	0.55	0.56
	(±1.77)	(±0.57)	(±1.55)	(±0.55)	(±0.85)	(±0.27)	(±0.58)	(±0.27)	(±1.43)	(±0.40)	(±0.18)	(±0.11)	(±0.12)	(±0.09)
2005	17.28	18.61	12.78	13.74	4.50	4.87	3.29	3.74	7.89	8.36	1.02	1.03	0.58	0.62
	(±1.82)	(±0.60)	(±1.61)	(±0.57)	(±0.85)	(±0.27)	(±0.59)	(±0.28)	(±1.49)	(±0.43)	(±0.18)	(±0.11)	(±0.15)	(±0.10)
2006	17.43	17.29	12.93	12.48	4.50	4.81	3.30	4.22	8.04	6.53	1.03	1.15	0.57	0.58
	(±1.84)	(±0.56)	(±1.64)	(±0.53)	(±0.85)	(±0.27)	(±0.59)	(±0.27)	(±1.51)	(±0.38)	(±0.19)	(±0.11)	(±0.13)	(±0.09)
2007	16.95	17.97	12.45	13.15	4.50	4.82	3.30	3.69	7.54	7.80	1.05	1.06	0.57	0.60
	(±1.78)	(±0.58)	(±1.56)	(±0.55)	(±0.85)	(±0.27)	(±0.59)	(±0.28)	(±1.43)	(±0.40)	(±0.19)	(±0.11)	(±0.13)	(±0.10)
2008	16.49	17.59	11.99	12.46	4.50	5.13	3.30	3.76	7.15	7.10	1.07	1.11	0.48	0.49
	(±1.70)	(±0.59)	(±1.48)	(±0.57)	(±0.85)	(±0.27)	(±0.59)	(±0.28)	(±1.34)	(±0.43)	(±0.19)	(±0.11)	(±0.12)	(±0.09)

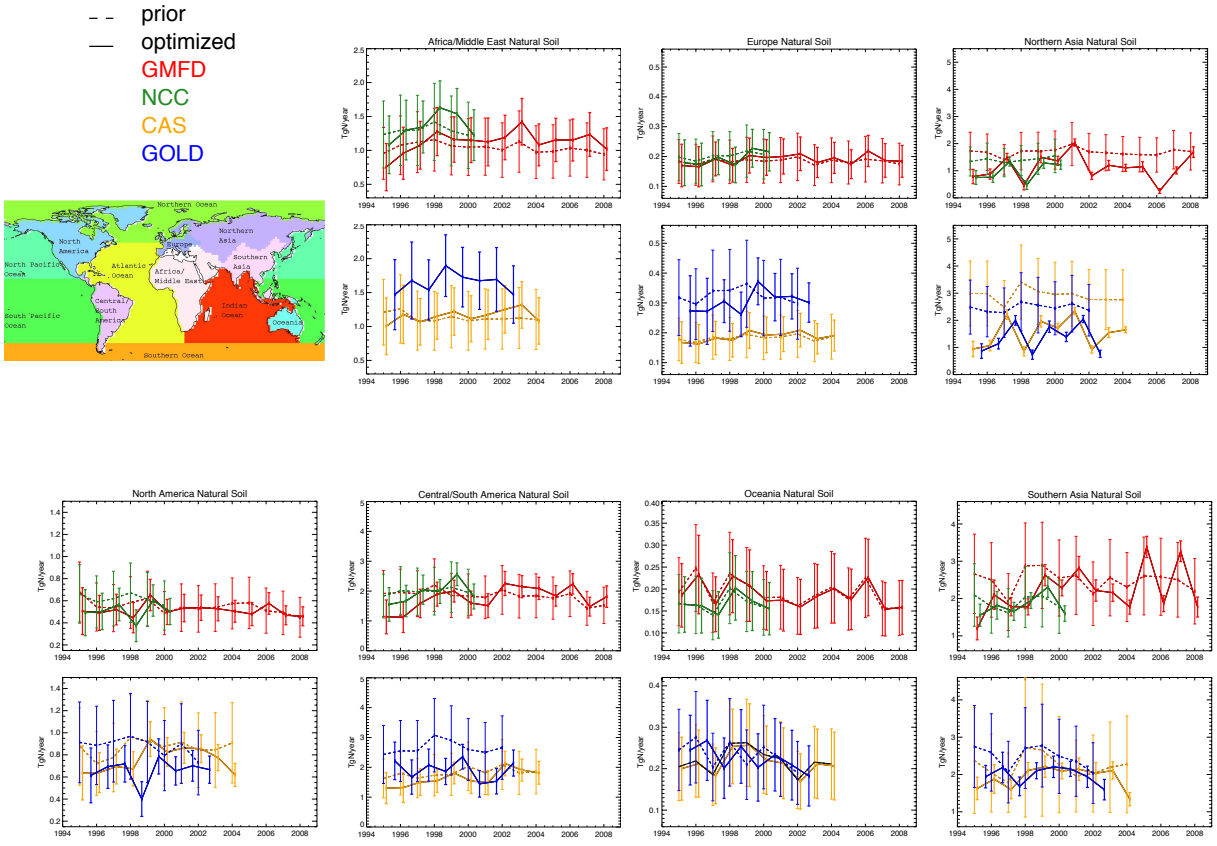

Fig. 3e. Comparison of prior (dash) and optimized (solid) natural soil emissions in $TgN_2O\text{-}N\,yr^{-1}$ from four inversions for seven regions, each using a different forcing data set for natural soil (red: GMFD; green: NCC; orange: CAS; and black: GOLD). Prior emissions uncertainties are 40 %, and posterior uncertainties are one standard deviation.

into multiple regions. The closer a given region is to a measurement site, the larger the sensitivity to emission perturbations in that region we would expect.

The seven land regions in this study are (1) Africa and Middle East; (2) Central and South America; (3) Northern Asia; (4) Southern Asia; (5) Europe; (6) North America; and (7) Oceania (see Fig. 3). Asia is divided into two, because there are multiple measurement stations in the region. This division within Asia is also of interest, because there is a high uncertainty in the winter soil emissions under snow and thawing conditions in the higher latitude regions (e.g., Groffman et al. (2006)) that apply to Russia, covered under "Northern Asia". China under "Southern Asia" is by far the largest consumer of nitrogen fertilizer between 1995 and 2008, as shown in Fig. 4 (International Fertilizer Industry Association, 2013). Its total nitrogen consumption is more than twice that of India, the second largest consumer since 2004 before the United States, and also under "Southern Asia". The six ocean regions in this study are (1) North Pacific; (2) South Pacific; (3) Northern Ocean; (4) Atlantic; (5) Southern Ocean; and (6) Indian Ocean (see Fig. 3).

We conduct regional inversions using four sets of a priori emissions for 1995 through 2008. The four sets differ only in natural soil emissions due to the different estimates that come from the four different forcing data sets used in the bottom-up estimates for this sector, and there is no difference in other sectors. We conduct an inversion using all measurements available, including AGAGE, NOAA, CSIRO, NIES, and Tohoku University networks. We find that by emission sector, the largest uncertainty reduction is for natural soil and, by region, it is for Northern Asia. We achieve these results because natural soil has the largest emissions among all sources and because we have the largest number of long-standing stations close to our Northern Asia region (see Fig. 1) that have high sensitivities. Figure 3 provides the prior and posterior emissions with uncertainty bars for all the sectors and regions quantified from this inversion, and Table 3 provides prior and posterior emissions with uncertainties for global total, global land, and total emissions by source sector. Table 4 lists prior and optimized emissions with uncertainties for each region, and Tables 5–9 provide prior and optimized emissions derived from this inversion for each sector and region using all the measurements. Some regional emissions by source sector can be constrained well, with a substantial reduction in posterior emissions uncertainty by using the measurements from different network stations between 1995 and 2008. However,

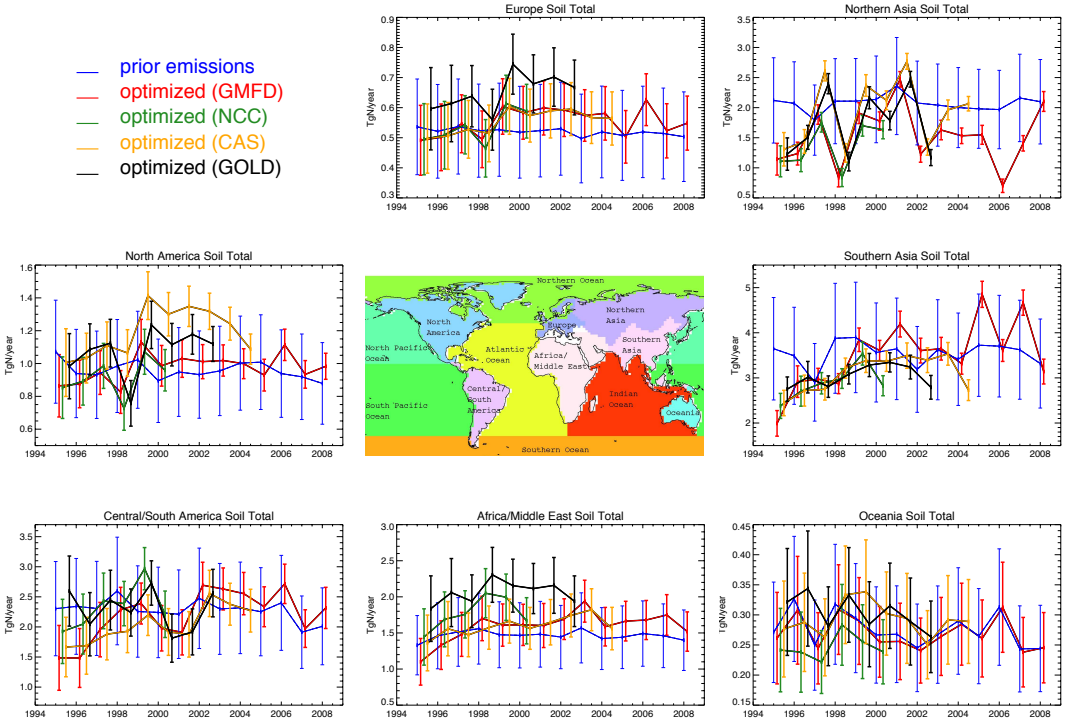

Fig. 3f. Comparison of prior (blue) and optimized total soil (natural + agricultural soil) emissions in $TgN_2O\text{-}N\,yr^{-1}$ from four inversions for seven regions, each using a different forcing data set for natural soil (red: GMFD; green: NCC; orange: CAS; and black: GOLD). Prior emissions uncertainties are 40 %, and posterior uncertainties are one standard deviation.

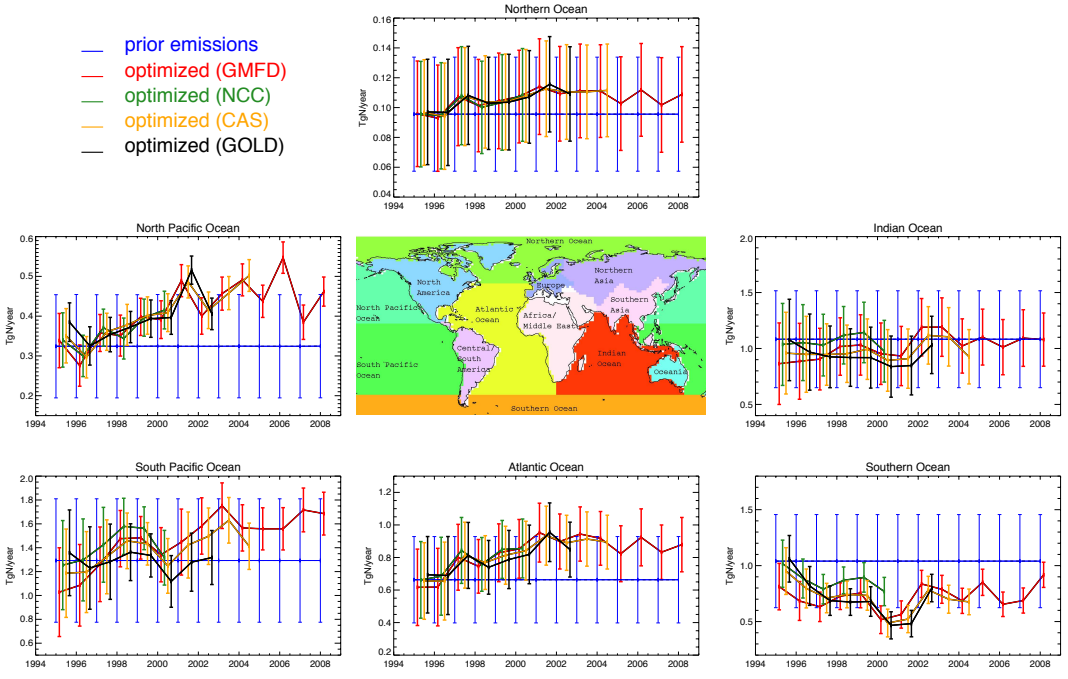

Fig. 3g. Comparison of prior (blue) and optimized ocean emissions in $TgN_2O\text{-}N\,yr^{-1}$ from four inversions for six regions, each using a different forcing data set for natural soil (red: GMFD; green: NCC; orange: CAS; and black: GOLD). Prior emissions uncertainties are 40 %, and posterior uncertainties are one standard deviation.

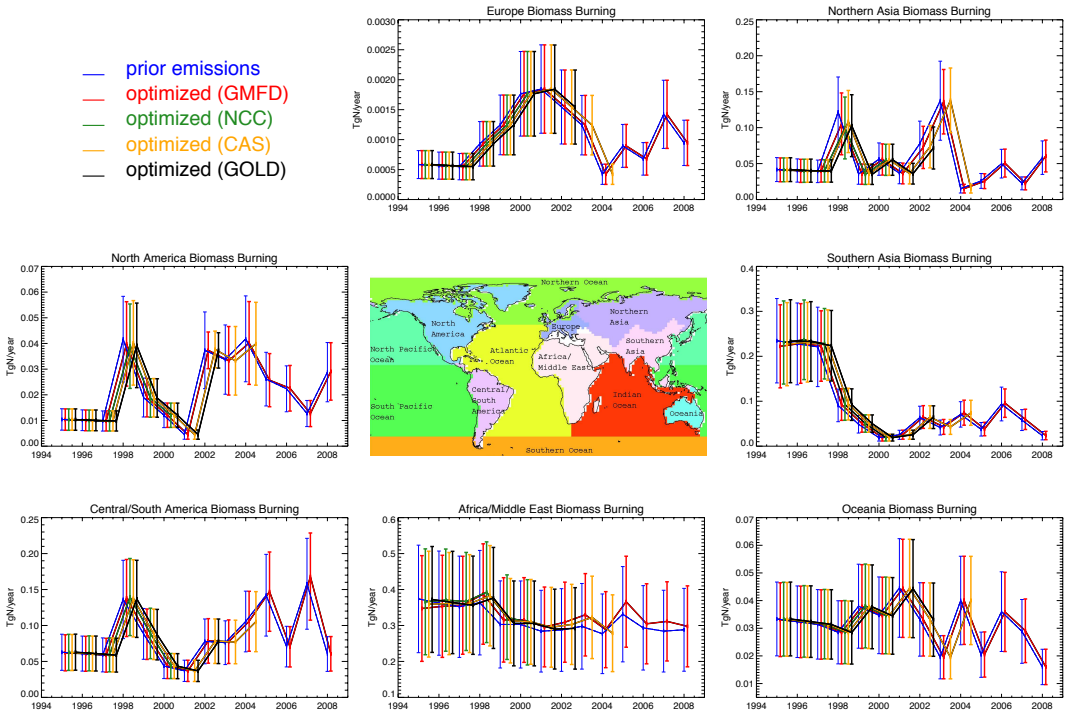

Fig. 3h. Comparison of prior (blue) and optimized biomass burning emissions in $TgN_2O\text{-}N\,yr^{-1}$ from four inversions for seven regions, each using a different forcing data set for natural soil (red: GMFD; green: NCC; orange: CAS; and black: GOLD). Prior emissions uncertainties are 40 %, and posterior uncertainties are one standard deviation.

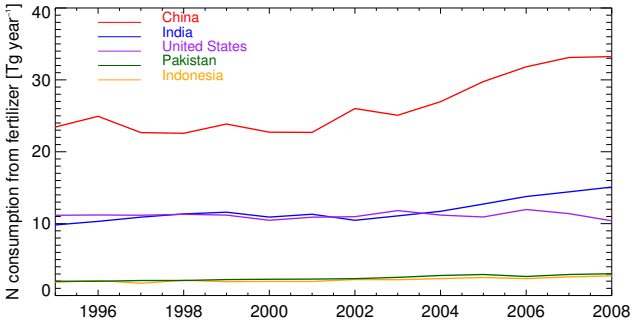

Fig. 4. Changes in nitrogen consumption from fertilizers by the top five consumers in the world in TgN $year^{-1}$(International Fertilizer Industry Association, 2013).

in other regions, especially for biomass burning emissions we see little uncertainty reduction due to the lack of observational data to constrain emissions at the sector and regional levels.

4.2 Emissions trend by source sector and region

We find a significant increase in global agricultural soil emissions (see Fig. 3a), and Southern Asia – the region that includes China and India – shows the most visible signal (see Fig. 3c and Table5). The 4-year mean agricultural soil emissions between 2005 and 2008 ($1.49 \pm 0.14\,TgN_2O\text{-}N\,yr^{-1}$) is 54 % greater than that from 1995 to 1998 ($0.97 \pm 0.12\,TgN_2O\text{-}N\,yr^{-1}$) for Southern Asia. We realize that there are anti-correlations contained and derived in state-vector error covariance matrix (**W**) in some of the estimates we find due to the nature of our inversion methodology. To find out how well observations could constrain emissions by sector and by region in our inversion, we calculated the average correlations (R) between optimized emissions (see Table S2 in the Supplement). High negative correlations indicate that these emissions are not well constrained, and we expect some neighboring regions and specific sectors to have emissions fall under this category due to the lack of nearby measurements in the current networks. Between Southern Asia's agricultural and natural soil emissions, the average correlation value is -0.36, showing some anti-correlation. This illustrates that we are unable to differentiate between the two source emissions (natural vs. agricultural), but given that this increasing trend still holds when we combine the agricultural and natural soil together in the region (see Fig. 3f), we are confident of the increasing soil N_2O emissions in Southern Asia. The 4-year mean total soil (including both natural and agricultural soil) emissions in this region between 2005 and 2008 ($4.1 \pm 0.27\,TgN_2O\text{-}N\,yr^{-1}$) is 52 % greater than the mean from 1995 to 1998 ($2.7 \pm 0.27\,TgN_2O\text{-}N\,yr^{-1}$).

There are nine cases where R values lie between -0.7 and -0.8. Eight of them are between agricultural soil and industrial emissions in Europe, and the remaining case is

Table 4. Prior and optimized regional total N_2O emissions with uncertainties using the GMFD forcing data sets for natural soil (TgN_2O-N yr^{-1}).

	North America		Central/South America		Europe		Africa/Middle East		Northern Asia		Southern Asia		Oceania	
Year	Prior	Posterior	Prior	Posterior	Prior	Posterior	Prior	Posterior	Prior	Posterior	Prior	Posterior	Prior	Posterior
1995	1.29	1.08	2.40	1.58	0.89	0.81	1.77	1.52	2.36	1.37	4.10	2.43	0.31	0.30
	(±0.49)	(±0.36)	(±0.62)	(±0.50)	(±0.44)	(±0.24)	(±0.38)	(±0.33)	(±0.58)	(±0.33)	(±0.96)	(±0.42)	(±0.12)	(±0.09)
1996	1.16	1.09	2.44	1.58	0.85	0.82	1.89	1.75	2.32	1.47	3.94	3.36	0.36	0.35
	(±0.48)	(±0.30)	(±0.60)	(±0.42)	(±0.44)	(±0.19)	(±0.39)	(±0.33)	(±0.56)	(±0.29)	(±0.93)	(±0.42)	(±0.13)	(±0.09)
1997	1.15	1.16	2.40	2.05	0.84	0.86	1.94	1.91	2.04	2.13	3.35	3.44	0.29	0.28
	(±0.48)	(±0.24)	(±0.58)	(±0.39)	(±0.44)	(±0.14)	(±0.40)	(±0.30)	(±0.50)	(±0.23)	(±0.81)	(±0.33)	(±0.11)	(±0.07)
1998	1.23	1.05	2.77	2.46	0.80	0.76	2.00	2.16	2.45	1.13	4.20	3.20	0.35	0.34
	(±0.48)	(±0.23)	(±0.64)	(±0.32)	(±0.44)	(±0.13)	(±0.41)	(±0.31)	(±0.57)	(±0.20)	(±1.01)	(±0.27)	(±0.12)	(±0.08)
1999	1.24	1.36	2.38	2.51	0.78	0.89	1.85	2.00	2.37	2.16	4.18	4.13	0.34	0.33
	(±0.48)	(±0.24)	(±0.55)	(±0.29)	(±0.44)	(±0.13)	(±0.38)	(±0.29)	(±0.57)	(±0.22)	(±1.01)	(±0.29)	(±0.11)	(±0.07)
2000	1.10	1.21	2.32	2.06	0.75	0.84	1.85	2.00	2.43	2.06	3.82	3.88	0.31	0.30
	(±0.47)	(±0.24)	(±0.54)	(±0.32)	(±0.43)	(±0.12)	(±0.37)	(±0.28)	(±0.58)	(±0.21)	(±0.94)	(±0.27)	(±0.11)	(±0.06)
2001	1.14	1.23	2.29	1.99	0.76	0.87	1.84	1.98	2.63	2.74	3.91	4.48	0.32	0.31
	(±0.48)	(±0.22)	(±0.53)	(±0.32)	(±0.44)	(±0.12)	(±0.37)	(±0.29)	(±0.63)	(±0.19)	(±0.95)	(±0.34)	(±0.11)	(±0.07)
2002	1.15	1.24	2.59	2.81	0.76	0.85	1.81	2.08	2.36	1.50	3.49	3.92	0.28	0.28
	(±0.47)	(±0.21)	(±0.60)	(±0.32)	(±0.44)	(±0.12)	(±0.36)	(±0.28)	(±0.56)	(±0.19)	(±0.85)	(±0.32)	(±0.11)	(±0.06)
2003	1.17	1.24	2.42	2.75	0.74	0.85	1.95	2.35	2.39	1.96	3.92	3.95	0.29	0.29
	(±0.48)	(±0.21)	(±0.54)	(±0.30)	(±0.43)	(±0.12)	(±0.39)	(±0.29)	(±0.56)	(±0.20)	(±0.94)	(±0.28)	(±0.11)	(±0.06)
2004	1.22	1.22	2.46	2.70	0.77	0.86	1.78	1.96	2.22	1.75	3.73	3.66	0.34	0.33
	(±0.48)	(±0.20)	(±0.55)	(±0.30)	(±0.44)	(±0.12)	(±0.36)	(±0.27)	(±0.54)	(±0.18)	(±0.89)	(±0.26)	(±0.11)	(±0.07)
2005	1.21	1.13	2.44	2.52	0.76	0.75	1.85	2.11	2.21	1.77	4.02	5.17	0.29	0.29
	(±0.48)	(±0.21)	(±0.53)	(±0.29)	(±0.44)	(±0.12)	(±0.37)	(±0.28)	(±0.54)	(±0.21)	(±0.96)	(±0.31)	(±0.11)	(±0.06)
2006	1.14	1.33	2.51	2.83	0.77	0.93	1.87	2.07	2.23	0.97	4.06	4.00	0.36	0.36
	(±0.47)	(±0.20)	(±0.56)	(±0.28)	(±0.44)	(±0.12)	(±0.37)	(±0.27)	(±0.54)	(±0.18)	(±0.95)	(±0.27)	(±0.12)	(±0.08)
2007	1.11	1.13	2.11	2.18	0.77	0.79	1.83	2.15	2.40	1.63	3.95	5.00	0.28	0.27
	(±0.47)	(±0.20)	(±0.44)	(±0.27)	(±0.44)	(±0.12)	(±0.37)	(±0.28)	(±0.58)	(±0.18)	(±0.94)	(±0.30)	(±0.11)	(±0.06)
2008	1.09	1.21	2.11	2.42	0.76	0.83	1.77	1.90	2.37	2.38	3.61	3.44	0.27	0.27
	(±0.47)	(±0.19)	(±0.46)	(±0.29)	(±0.44)	(±0.12)	(±0.35)	(±0.28)	(±0.57)	(±0.21)	(±0.87)	(±0.30)	(±0.12)	(±0.12)

Table 5. Prior and optimized regional agricultural soil N_2O emissions with uncertainties using the GMFD forcing data sets for natural soil (GgN_2O-N yr^{-1})

	North America		Central/South America		Europe		Africa/Middle East		Northern Asia		Southern Asia		Oceania	
Year	Prior	Posterior	Prior	Posterior	Prior	Posterior	Prior	Posterior	Prior	Posterior	Prior	Posterior	Prior	Posterior
1995	392.79	358.38	384.31	349.92	352.78	321.60	374.48	347.15	392.02	355.21	984.61	793.39	77.17	75.69
	(±157.12)	(±148.40)	(±153.72)	(±152.56)	(±141.11)	(±116.27)	(±149.79)	(±147.62)	(±156.81)	(±145.40)	(±393.85)	(±221.00)	(±30.87)	(±29.04)
1996	395.51	385.30	388.49	357.64	348.97	335.57	383.18	372.91	388.78	358.24	990.30	814.22	78.93	74.64
	(±158.20)	(±147.55)	(±155.40)	(±153.55)	(±139.59)	(±114.77)	(±153.27)	(±150.90)	(±155.51)	(±145.77)	(±396.12)	(±242.87)	(±31.57)	(±28.99)
1997	398.23	425.15	392.68	367.69	345.16	354.27	391.89	404.01	385.55	411.69	995.99	1189.49	80.68	79.16
	(±159.29)	(±129.19)	(±157.07)	(±153.90)	(±138.06)	(±96.11)	(±156.76)	(±148.25)	(±154.22)	(±129.05)	(±398.40)	(±209.24)	(±32.27)	(±28.70)
1998	400.95	379.73	396.86	388.27	341.35	323.75	400.60	422.89	382.31	371.85	1001.68	1095.26	82.44	79.56
	(±160.38)	(±121.81)	(±158.75)	(±155.00)	(±136.54)	(±92.78)	(±160.24)	(±144.70)	(±152.93)	(±114.37)	(±400.67)	(±191.52)	(±32.97)	(±29.14)
1999	403.67	479.82	401.05	390.04	337.54	400.47	409.30	448.11	379.08	411.13	1007.37	1216.61	84.19	82.05
	(±161.47)	(±129.01)	(±160.42)	(±156.68)	(±135.01)	(±91.75)	(±163.72)	(±149.37)	(±151.63)	(±121.28)	(±402.95)	(±200.46)	(±33.68)	(±32.45)
2000	406.39	487.99	405.23	381.43	333.73	386.20	418.01	460.82	375.84	411.84	1013.06	1321.98	85.95	81.96
	(±162.55)	(±128.35)	(±162.09)	(±158.04)	(±133.49)	(±87.64)	(±167.20)	(±149.60)	(±150.34)	(±116.62)	(±405.22)	(±197.23)	(±34.38)	(±32.50)
2001	410.88	496.28	420.97	395.77	335.24	398.65	427.37	477.52	377.27	431.64	1023.52	1372.71	86.53	81.28
	(±164.35)	(±112.14)	(±168.39)	(±163.99)	(±134.09)	(±87.21)	(±170.95)	(±151.33)	(±150.91)	(±119.44)	(±409.41)	(±209.14)	(±34.61)	(±32.99)
2002	405.93	474.33	435.23	439.68	331.20	382.79	438.24	501.02	379.15	413.74	1059.72	1390.01	83.56	81.43
	(±162.37)	(±94.00)	(±174.09)	(±169.03)	(±132.48)	(±87.10)	(±175.30)	(±155.96)	(±151.66)	(±122.40)	(±423.89)	(±222.21)	(±33.42)	(±32.14)
2003	416.95	491.11	470.95	483.82	326.35	393.69	439.54	517.54	378.27	426.42	1063.99	1488.29	82.56	80.46
	(±166.78)	(±80.98)	(±188.38)	(±181.07)	(±130.54)	(±84.69)	(±175.82)	(±155.29)	(±151.31)	(±121.48)	(±425.59)	(±234.32)	(±33.03)	(±31.47)
2004	426.63	494.00	475.54	463.94	331.82	385.39	448.24	505.17	383.50	423.84	1104.59	1544.70	85.87	83.08
	(±170.65)	(±85.38)	(±190.22)	(±180.86)	(±132.73)	(±89.46)	(±179.30)	(±156.87)	(±153.40)	(±125.48)	(±441.84)	(±231.67)	(±34.35)	(±31.81)
2005	427.76	449.73	488.15	496.70	327.85	328.61	456.09	509.13	386.30	398.82	1119.44	1469.05	87.41	84.35
	(±171.10)	(±89.64)	(±195.26)	(±184.92)	(±131.14)	(±88.44)	(±182.43)	(±158.06)	(±154.52)	(±124.51)	(±447.77)	(±250.02)	(±34.96)	(±31.79)
2006	428.06	538.10	488.49	473.53	328.08	407.78	456.41	526.03	386.57	449.32	1120.22	1742.11	87.47	86.48
	(±171.22)	(±90.21)	(±195.40)	(±184.55)	(±131.23)	(±85.86)	(±182.56)	(±156.06)	(±154.63)	(±122.95)	(±448.09)	(±227.32)	(±34.99)	(±32.82)
2007	428.36	465.63	488.83	493.78	328.31	335.98	456.73	513.43	386.84	394.76	1121.00	1398.79	87.53	84.09
	(±171.34)	(±85.25)	(±195.53)	(±186.09)	(±131.33)	(±88.94)	(±182.69)	(±154.57)	(±154.74)	(±120.90)	(±448.40)	(±241.54)	(±35.01)	(±31.74)
2008	428.66	523.77	489.18	501.05	328.54	364.62	457.05	499.95	387.11	414.38	1121.79	1367.61	87.59	87.29
	(±171.46)	(±78.96)	(±195.67)	(±186.79)	(±131.42)	(±89.30)	(±182.82)	(±156.60)	(±154.84)	(±119.92)	(±448.72)	(±244.52)	(±35.04)	(±32.12)

between the natural soil source in Northern and Southern Asia in 2006, when Northern Asian natural soil emission estimates are very low. The average correlation between European agricultural soil and industrial emissions was −0.66, and between Northern and Southern Asian natural soil emissions, it was −0.39. However, more than 98.8 % of the absolute R values are less than 0.3, and the average correlation value between all regions was −0.0061. The following are

Table 6. Prior and optimized regional industrial N_2O emissions with uncertainties using the GMFD forcing data sets for natural soil (GgN_2O-N yr^{-1})

	North America		Central/South America		Europe		Africa/Middle East		Northern Asia		Southern Asia		Oceania	
Year	Prior	Posterior	Prior	Posterior	Prior	Posterior	Prior	Posterior	Prior	Posterior	Prior	Posterior	Prior	Posterior
1995	212.15	202.04	33.87	33.60	353.20	319.20	69.23	68.31	196.83	187.35	222.48	213.88	4.93	4.93
	(± 84.86)	(± 83.45)	(± 13.55)	(± 13.55)	(± 141.28)	(± 118.51)	(± 27.69)	(± 27.68)	(± 78.73)	(± 76.83)	(± 88.99)	(± 83.15)	(± 1.97)	(± 1.97)
1996	209.14	206.64	34.74	34.50	327.90	314.59	70.48	70.14	203.89	195.61	225.85	212.64	5.21	5.19
	(± 83.66)	(± 81.92)	(± 13.90)	(± 13.89)	(± 131.16)	(± 111.47)	(± 28.19)	(± 28.18)	(± 81.55)	(± 79.42)	(± 90.34)	(± 83.13)	(± 2.08)	(± 2.08)
1997	206.13	205.73	35.61	35.41	302.61	311.72	71.73	72.20	210.94	201.93	229.21	242.34	5.49	5.48
	(± 82.45)	(± 74.77)	(± 14.24)	(± 14.24)	(± 121.04)	(± 94.40)	(± 28.69)	(± 28.59)	(± 84.37)	(± 56.12)	(± 91.69)	(± 84.06)	(± 2.19)	(± 2.19)
1998	203.12	187.98	36.47	36.42	277.31	268.81	72.98	73.74	217.99	188.62	232.58	234.31	5.76	5.75
	(± 81.25)	(± 72.26)	(± 14.59)	(± 14.59)	(± 110.93)	(± 85.33)	(± 29.19)	(± 28.98)	(± 87.19)	(± 57.14)	(± 93.03)	(± 84.44)	(± 2.31)	(± 2.30)
1999	200.11	214.09	37.34	37.25	252.02	289.40	74.24	75.79	225.04	220.28	235.95	237.12	6.04	6.03
	(± 80.04)	(± 66.52)	(± 14.94)	(± 14.93)	(± 100.81)	(± 81.08)	(± 29.69)	(± 29.49)	(± 90.02)	(± 60.86)	(± 94.38)	(± 87.77)	(± 2.42)	(± 2.42)
2000	197.10	209.49	38.21	38.02	226.73	252.00	75.49	77.22	232.09	226.52	239.32	249.20	6.32	6.30
	(± 78.84)	(± 65.15)	(± 15.28)	(± 15.28)	(± 90.69)	(± 74.87)	(± 30.19)	(± 29.88)	(± 92.84)	(± 60.39)	(± 95.73)	(± 87.88)	(± 2.53)	(± 2.53)
2001	183.93	198.27	38.78	38.60	236.17	269.18	75.65	77.63	230.97	236.65	244.16	262.10	6.15	6.12
	(± 73.57)	(± 61.83)	(± 15.51)	(± 15.51)	(± 94.47)	(± 74.90)	(± 30.26)	(± 30.02)	(± 92.39)	(± 58.89)	(± 97.66)	(± 90.06)	(± 2.46)	(± 2.46)
2002	180.49	192.02	38.73	38.79	228.99	253.78	75.47	77.63	203.01	200.43	239.57	251.82	5.86	5.85
	(± 72.19)	(± 58.44)	(± 15.49)	(± 15.49)	(± 91.60)	(± 73.61)	(± 30.19)	(± 29.97)	(± 81.20)	(± 52.64)	(± 95.83)	(± 91.75)	(± 2.34)	(± 2.34)
2003	176.93	183.98	39.43	39.55	240.11	277.44	79.04	81.92	206.90	200.13	250.23	263.40	6.47	6.45
	(± 70.77)	(± 57.51)	(± 15.77)	(± 15.77)	(± 96.04)	(± 75.99)	(± 31.62)	(± 31.33)	(± 82.76)	(± 52.39)	(± 100.09)	(± 92.97)	(± 2.59)	(± 2.59)
2004	174.25	179.52	40.57	40.51	247.50	279.28	78.60	80.69	208.02	207.37	250.86	273.88	6.70	6.68
	(± 69.70)	(± 58.87)	(± 16.23)	(± 16.22)	(± 99.00)	(± 78.44)	(± 31.44)	(± 31.16)	(± 83.21)	(± 57.22)	(± 100.34)	(± 92.90)	(± 2.68)	(± 2.68)
2005	171.79	173.20	41.35	41.43	247.65	248.10	80.97	82.76	208.18	196.15	259.68	276.33	7.08	7.06
	(± 68.72)	(± 57.82)	(± 16.54)	(± 16.53)	(± 99.06)	(± 77.72)	(± 32.39)	(± 32.07)	(± 83.27)	(± 57.86)	(± 103.87)	(± 95.45)	(± 2.83)	(± 2.83)
2006	174.57	191.57	42.02	41.94	251.67	300.46	82.29	85.07	211.56	222.76	263.89	297.87	7.19	7.18
	(± 69.83)	(± 58.52)	(± 16.81)	(± 16.80)	(± 100.67)	(± 77.24)	(± 32.91)	(± 32.56)	(± 84.62)	(± 59.26)	(± 105.55)	(± 96.93)	(± 2.88)	(± 2.88)
2007	177.40	181.14	42.70	42.76	255.74	262.54	83.62	85.64	214.98	201.96	268.16	274.59	7.31	7.28
	(± 70.96)	(± 57.09)	(± 17.08)	(± 17.07)	(± 102.30)	(± 77.00)	(± 33.45)	(± 33.04)	(± 85.99)	(± 55.40)	(± 107.26)	(± 97.00)	(± 2.92)	(± 2.92)
2008	180.28	194.13	43.39	43.51	259.89	284.64	84.97	86.74	218.47	216.52	272.50	279.06	7.43	7.42
	(± 72.11)	(± 56.81)	(± 17.36)	(± 17.35)	(± 103.95)	(± 79.40)	(± 33.99)	(± 33.58)	(± 87.39)	(± 59.83)	(± 109.00)	(± 99.83)	(± 2.97)	(± 2.97)

Table 7. Prior and optimized regional natural soil N_2O emissions with uncertainties using the GMFD forcing data sets for natural soil (GgN_2O-N yr^{-1})

	North America		Central/South America		Europe		Africa/Middle East		Northern Asia		Southern Asia		Oceania	
Year	Prior	Posterior	Prior	Posterior	Prior	Posterior	Prior	Posterior	Prior	Posterior	Prior	Posterior	Prior	Posterior
1995	679.29	505.88	1919.51	1135.93	183.39	169.94	955.68	753.30	1728.21	787.78	2661.23	1198.60	193.88	185.67
	(± 271.72)	(± 211.65)	(± 767.80)	(± 565.93)	(± 73.36)	(± 71.35)	(± 382.27)	(± 347.29)	(± 691.29)	(± 265.25)	(± 1064.49)	(± 305.46)	(± 77.55)	(± 72.38)
1996	543.66	489.87	1952.74	1126.16	172.38	165.75	1077.90	958.05	1682.49	878.30	2498.97	2102.67	247.64	233.06
	(± 217.46)	(± 158.26)	(± 781.10)	(± 513.81)	(± 68.95)	(± 67.08)	(± 431.16)	(± 383.99)	(± 672.99)	(± 188.72)	(± 999.59)	(± 392.94)	(± 99.05)	(± 89.42)
1997	533.19	519.95	1914.88	1587.33	192.10	192.07	1121.76	1076.03	1407.43	1473.52	1905.82	1782.61	169.08	165.31
	(± 213.28)	(± 138.65)	(± 765.95)	(± 476.91)	(± 76.84)	(± 56.72)	(± 448.70)	(± 352.02)	(± 562.97)	(± 168.30)	(± 762.33)	(± 246.09)	(± 67.63)	(± 62.44)
1998	583.93	446.88	2200.40	1896.80	182.21	171.07	1158.40	1277.62	1725.19	462.80	2875.57	1776.61	235.18	229.25
	(± 233.57)	(± 137.30)	(± 880.16)	(± 402.20)	(± 72.89)	(± 56.31)	(± 463.36)	(± 355.32)	(± 690.08)	(± 166.57)	(± 1150.23)	(± 216.06)	(± 94.07)	(± 83.11)
1999	619.21	651.51	1855.17	1998.89	189.12	203.40	1065.73	1160.88	1729.30	1497.60	2889.03	2628.07	210.43	207.79
	(± 247.69)	(± 142.23)	(± 742.07)	(± 365.48)	(± 75.65)	(± 58.61)	(± 426.29)	(± 334.23)	(± 691.72)	(± 200.40)	(± 1155.61)	(± 284.09)	(± 84.17)	(± 81.42)
2000	488.51	498.20	1835.96	1596.70	184.59	196.75	1048.75	1151.04	1761.80	1365.30	2550.00	2285.15	180.65	173.23
	(± 195.40)	(± 113.78)	(± 734.38)	(± 402.85)	(± 73.83)	(± 59.76)	(± 419.50)	(± 330.61)	(± 704.72)	(± 170.79)	(± 1020.00)	(± 211.73)	(± 72.26)	(± 66.75)
2001	537.48	534.20	1790.40	1514.08	188.33	200.30	1054.77	1125.35	1981.75	2038.99	2620.00	2819.69	181.36	174.65
	(± 214.99)	(± 124.17)	(± 716.16)	(± 399.76)	(± 75.33)	(± 58.80)	(± 421.91)	(± 352.78)	(± 792.70)	(± 131.23)	(± 1048.00)	(± 310.16)	(± 72.54)	(± 70.18)
2002	526.63	537.09	2040.23	2253.90	198.86	209.24	1004.89	1190.08	1698.17	812.74	2128.59	2215.26	161.68	159.29
	(± 210.65)	(± 114.42)	(± 816.09)	(± 404.99)	(± 79.54)	(± 56.33)	(± 401.95)	(± 328.22)	(± 679.27)	(± 132.90)	(± 851.44)	(± 286.33)	(± 64.67)	(± 62.67)
2003	538.01	527.31	1828.63	2147.18	171.15	180.24	1130.62	1422.17	1664.21	1201.81	2559.41	2157.87	184.65	183.73
	(± 215.21)	(± 109.25)	(± 731.45)	(± 368.94)	(± 68.46)	(± 50.39)	(± 452.25)	(± 343.22)	(± 665.68)	(± 179.34)	(± 1023.76)	(± 231.93)	(± 73.86)	(± 72.25)
2004	575.77	504.99	1841.38	2089.88	187.39	195.64	973.61	1081.38	1617.60	1108.54	2308.74	1770.00	203.97	201.48
	(± 230.31)	(± 99.01)	(± 736.55)	(± 372.06)	(± 74.96)	(± 52.01)	(± 389.45)	(± 308.31)	(± 647.04)	(± 128.37)	(± 923.49)	(± 187.75)	(± 81.59)	(± 78.97)
2005	580.68	479.49	1764.26	1838.49	180.02	174.39	984.32	1154.59	1594.23	1149.54	2604.91	3382.42	177.26	176.47
	(± 232.27)	(± 104.91)	(± 705.70)	(± 344.05)	(± 72.01)	(± 48.26)	(± 393.73)	(± 319.42)	(± 637.69)	(± 184.05)	(± 1041.96)	(± 285.43)	(± 70.90)	(± 68.86)
2006	510.65	575.78	1911.59	2242.29	191.30	218.67	1034.90	1153.08	1582.08	252.16	2582.92	1864.81	225.55	226.20
	(± 204.26)	(± 97.43)	(± 764.64)	(± 340.38)	(± 76.52)	(± 52.19)	(± 413.96)	(± 309.57)	(± 632.83)	(± 90.56)	(± 1033.17)	(± 215.28)	(± 90.22)	(± 87.19)
2007	490.94	468.16	1423.59	1478.66	185.84	187.00	1004.34	1235.62	1774.55	1012.47	2502.80	3268.43	155.95	153.94
	(± 196.38)	(± 85.67)	(± 569.43)	(± 315.16)	(± 74.34)	(± 56.28)	(± 401.74)	(± 322.86)	(± 709.82)	(± 130.52)	(± 1001.12)	(± 277.77)	(± 62.38)	(± 60.82)
2008	450.18	459.46	1520.81	1814.89	174.95	183.99	942.36	1019.16	1711.16	1688.31	2196.15	1772.59	156.60	158.16
	(± 180.07)	(± 85.37)	(± 608.32)	(± 360.17)	(± 69.98)	(± 53.42)	(± 376.95)	(± 313.83)	(± 684.46)	(± 193.06)	(± 878.46)	(± 267.77)	(± 62.64)	(± 61.44)

the emission sources and regions that show negative correlation values between −0.35 and −0.7 that were not mentioned above: Southern Ocean and Indian Ocean; South Pacific and Central/South America Natural Soil; Southern Asia Agricultural Soil and Industrial; North America Agricultural and Natural Soil; Africa/Middle East and Central/South America Natural Soil; Africa/Middle East and Southern Asia Natural Soil; Northern Asia and North America Natural Soil. We therefore emphasize that total emissions are a robust result but emissions by source sector and region have much larger uncertainties and some emissions by region and sector (listed above) are not well constrained.

Table 8. Prior and optimized regional ocean N_2O emissions with uncertainties using the GMFD forcing data sets for natural soil (GgN_2O-N yr^{-1})

	North Pacific		South Pacific		Northern Ocean		Atlantic		Southern Ocean		Indian Ocean	
Year	Prior	Posterior	Prior	Posterior	Prior	Posterior	Prior	Posterior	Prior	Posterior	Prior	Posterior
1995	324.27	338.60	1292.88	1027.80	95.58	95.84	663.28	616.69	1040.35	812.41	1082.73	864.04
	(± 129.71)	(± 68.26)	(± 517.15)	(± 372.03)	(± 38.23)	(± 35.38)	(± 265.31)	(± 234.73)	(± 416.14)	(± 207.73)	(± 433.09)	(± 364.29)
1996	324.58	275.74	1292.83	1085.26	95.57	92.90	663.32	617.96	1040.09	684.09	1082.70	885.62
	(± 129.83)	(± 51.88)	(± 517.13)	(± 341.91)	(± 38.23)	(± 35.61)	(± 265.33)	(± 238.29)	(± 416.04)	(± 173.86)	(± 433.08)	(± 339.30)
1997	324.27	357.72	1292.88	1261.18	95.58	107.31	663.28	801.34	1040.35	631.78	1082.73	904.84
	(± 129.71)	(± 46.49)	(± 517.15)	(± 312.72)	(± 38.23)	(± 32.85)	(± 265.31)	(± 202.32)	(± 416.14)	(± 131.63)	(± 433.09)	(± 275.49)
1998	324.27	351.16	1292.88	1476.02	95.58	101.33	663.28	745.68	1040.35	726.68	1082.73	1017.48
	(± 129.71)	(± 51.51)	(± 517.15)	(± 236.06)	(± 38.23)	(± 30.97)	(± 265.31)	(± 164.87)	(± 416.14)	(± 119.04)	(± 433.09)	(± 256.93)
1999	324.27	398.21	1292.88	1483.16	95.58	104.49	663.28	828.91	1040.35	755.47	1082.73	1031.50
	(± 129.71)	(± 46.77)	(± 517.15)	(± 178.37)	(± 38.23)	(± 32.06)	(± 265.31)	(± 177.70)	(± 416.14)	(± 132.24)	(± 433.09)	(± 269.88)
2000	324.58	391.21	1292.83	1341.18	95.57	107.36	663.32	853.22	1040.09	516.52	1082.70	953.14
	(± 129.83)	(± 47.45)	(± 517.13)	(± 227.28)	(± 38.23)	(± 31.06)	(± 265.33)	(± 180.38)	(± 416.04)	(± 123.77)	(± 433.08)	(± 274.84)
2001	324.27	489.20	1292.88	1447.38	95.58	114.04	663.28	952.69	1040.35	563.14	1082.73	932.55
	(± 129.71)	(± 40.28)	(± 517.15)	(± 276.54)	(± 38.23)	(± 32.07)	(± 265.31)	(± 180.95)	(± 416.14)	(± 121.83)	(± 433.09)	(± 264.76)
2002	324.27	400.48	1292.88	1582.19	95.58	109.25	663.28	898.33	1040.35	836.36	1082.73	1189.84
	(± 129.71)	(± 45.89)	(± 517.15)	(± 236.24)	(± 38.23)	(± 31.73)	(± 265.31)	(± 169.01)	(± 416.14)	(± 121.49)	(± 433.09)	(± 256.65)
2003	324.27	456.63	1292.88	1752.11	95.58	111.19	663.28	944.19	1040.35	788.24	1082.73	1191.07
	(± 129.71)	(± 41.59)	(± 517.15)	(± 191.25)	(± 38.23)	(± 31.40)	(± 265.31)	(± 166.73)	(± 416.14)	(± 124.89)	(± 433.09)	(± 261.40)
2004	324.58	491.22	1292.83	1566.13	95.57	111.04	663.32	917.45	1040.09	685.36	1082.70	1022.33
	(± 129.83)	(± 40.21)	(± 517.13)	(± 193.83)	(± 38.23)	(± 31.07)	(± 265.33)	(± 165.07)	(± 416.04)	(± 112.60)	(± 433.08)	(± 242.50)
2005	324.27	437.36	1292.88	1558.18	95.58	102.67	663.28	823.05	1040.35	850.91	1082.73	1101.84
	(± 129.71)	(± 40.54)	(± 517.15)	(± 176.45)	(± 38.23)	(± 31.38)	(± 265.31)	(± 171.79)	(± 416.14)	(± 117.30)	(± 433.09)	(± 249.93)
2006	324.27	547.16	1292.88	1558.47	95.58	111.87	663.28	923.72	1040.35	654.50	1082.73	1011.76
	(± 129.71)	(± 39.46)	(± 517.15)	(± 177.21)	(± 38.23)	(± 31.09)	(± 265.31)	(± 175.05)	(± 416.14)	(± 109.42)	(± 433.09)	(± 246.71)
2007	324.27	384.74	1292.88	1716.63	95.58	101.75	663.28	832.44	1040.35	688.13	1082.73	1093.18
	(± 129.71)	(± 43.21)	(± 517.15)	(± 183.55)	(± 38.23)	(± 31.71)	(± 265.31)	(± 167.27)	(± 416.14)	(± 112.33)	(± 433.09)	(± 252.95)
2008	324.58	461.74	1292.83	1685.77	95.57	108.83	663.32	878.97	1040.09	917.89	1082.70	1079.39
	(± 129.83)	(± 36.63)	(± 517.13)	(± 179.28)	(± 38.23)	(± 32.02)	(± 265.33)	(± 166.93)	(± 416.04)	(± 112.67)	(± 433.08)	(± 237.85)

Table 9. Prior and optimized regional biomass burning N_2O emissions with uncertainties using the GMFD forcing data sets for natural soil (GgN_2O-N yr^{-1}).

	North America		Central/South America		Europe		Africa/Middle East		Northern Asia		Southern Asia		Oceania	
Year	Prior	Posterior	Prior	Posterior	Prior	Posterior	Prior	Posterior	Prior	Posterior	Prior	Posterior	Prior	Posterior
1995	10.41	10.36	62.76	61.96	0.58	0.58	373.89	347.24	41.65	41.29	234.64	222.18	33.36	33.09
	(± 4.16)	(± 4.16)	(± 25.10)	(± 25.08)	(± 0.23)	(± 0.23)	(± 149.56)	(± 147.01)	(± 16.66)	(± 16.56)	(± 93.86)	(± 92.39)	(± 13.34)	(± 13.34)
1996	10.10	10.05	60.90	60.65	0.57	0.57	362.14	353.28	40.40	39.90	227.62	228.59	32.36	32.29
	(± 4.04)	(± 4.04)	(± 24.36)	(± 24.31)	(± 0.23)	(± 0.23)	(± 144.86)	(± 141.99)	(± 16.16)	(± 16.07)	(± 91.05)	(± 88.60)	(± 12.94)	(± 12.93)
1997	9.80	9.83	59.09	58.67	0.55	0.55	352.06	356.26	39.22	39.78	220.94	222.86	31.41	31.36
	(± 3.92)	(± 3.92)	(± 23.64)	(± 23.55)	(± 0.22)	(± 0.22)	(± 140.82)	(± 136.22)	(± 15.69)	(± 15.52)	(± 88.38)	(± 78.36)	(± 12.57)	(± 12.55)
1998	41.68	39.83	136.18	138.18	0.93	0.93	363.41	387.49	121.74	105.26	90.71	92.63	28.53	28.51
	(± 16.67)	(± 16.43)	(± 54.47)	(± 53.60)	(± 0.37)	(± 0.37)	(± 145.37)	(± 139.67)	(± 48.70)	(± 42.99)	(± 36.28)	(± 35.19)	(± 11.41)	(± 11.40)
1999	18.95	18.89	88.35	87.82	1.25	1.25	302.91	315.55	35.46	35.28	48.77	50.43	37.97	37.84
	(± 7.58)	(± 7.49)	(± 35.34)	(± 35.09)	(± 0.50)	(± 0.50)	(± 121.17)	(± 117.37)	(± 14.18)	(± 14.09)	(± 19.51)	(± 19.33)	(± 15.19)	(± 15.15)
2000	12.03	12.06	43.59	43.58	1.76	1.77	302.77	315.19	56.24	55.71	18.94	19.05	34.68	34.60
	(± 4.81)	(± 4.74)	(± 17.44)	(± 17.42)	(± 0.71)	(± 0.71)	(± 121.11)	(± 117.85)	(± 22.50)	(± 21.65)	(± 7.58)	(± 7.57)	(± 13.87)	(± 13.85)
2001	4.51	4.51	36.96	36.92	1.84	1.84	284.17	295.91	36.55	36.24	25.29	25.54	44.57	44.42
	(± 1.80)	(± 1.80)	(± 14.78)	(± 14.77)	(± 0.74)	(± 0.74)	(± 113.67)	(± 111.00)	(± 14.62)	(± 14.42)	(± 10.12)	(± 10.10)	(± 17.83)	(± 17.74)
2002	37.34	37.33	77.88	78.55	1.54	1.54	287.42	309.13	77.88	72.50	63.53	64.90	33.19	33.21
	(± 14.94)	(± 7.14)	(± 31.15)	(± 30.97)	(± 0.62)	(± 0.62)	(± 114.97)	(± 111.39)	(± 31.15)	(± 29.37)	(± 25.41)	(± 25.29)	(± 13.28)	(± 13.25)
2003	33.72	33.25	76.05	77.46	1.24	1.24	297.74	329.73	137.45	136.06	41.53	42.88	19.50	19.52
	(± 13.49)	(± 13.34)	(± 30.42)	(± 30.29)	(± 0.50)	(± 0.50)	(± 119.09)	(± 114.56)	(± 54.98)	(± 44.82)	(± 16.61)	(± 16.53)	(± 7.80)	(± 7.80)
2004	41.80	40.19	105.55	105.88	0.42	0.42	276.91	288.37	15.15	15.14	70.70	74.51	40.03	40.10
	(± 16.72)	(± 16.13)	(± 42.22)	(± 41.66)	(± 0.17)	(± 0.17)	(± 110.76)	(± 105.74)	(± 6.06)	(± 6.05)	(± 28.28)	(± 27.83)	(± 16.01)	(± 15.94)
2005	26.11	25.70	142.09	147.05	0.90	0.90	331.32	366.11	25.89	25.52	37.60	38.16	20.43	20.50
	(± 10.45)	(± 10.35)	(± 56.84)	(± 55.15)	(± 0.36)	(± 0.36)	(± 132.53)	(± 126.55)	(± 10.35)	(± 10.32)	(± 15.04)	(± 14.98)	(± 8.17)	(± 8.17)
2006	22.34	22.55	70.62	70.37	0.68	0.68	293.43	304.68	49.91	50.70	93.86	95.78	36.01	35.90
	(± 8.94)	(± 8.88)	(± 28.25)	(± 28.05)	(± 0.27)	(± 0.27)	(± 117.37)	(± 111.33)	(± 19.97)	(± 19.42)	(± 37.54)	(± 31.60)	(± 14.41)	(± 14.32)
2007	12.72	12.70	158.00	168.02	1.42	1.42	284.28	311.38	22.50	22.45	58.04	59.69	28.86	29.09
	(± 5.09)	(± 5.08)	(± 63.20)	(± 60.62)	(± 0.57)	(± 0.57)	(± 113.71)	(± 110.16)	(± 9.00)	(± 8.98)	(± 23.22)	(± 22.57)	(± 11.54)	(± 11.50)
2008	28.82	29.11	60.27	60.58	0.95	0.95	288.02	297.60	58.24	60.54	23.35	23.74	16.00	16.02
	(± 11.53)	(± 11.19)	(± 24.11)	(± 24.01)	(± 0.38)	(± 0.38)	(± 115.21)	(± 112.60)	(± 23.30)	(± 22.13)	(± 9.34)	(± 9.32)	(± 6.40)	(± 6.40)

Figure 3a also illustrates that the optimized emissions using the GOLD forcing data set still produces substantially different results up to 1997 for global total, global land, and global natural soil, illustrating that the uncertainty is underestimated for the earlier time periods, and that the emissions are not very well constrained. However in later years, the optimized natural soil emissions converge in North America, Central/South America, Africa/Middle East, Northern

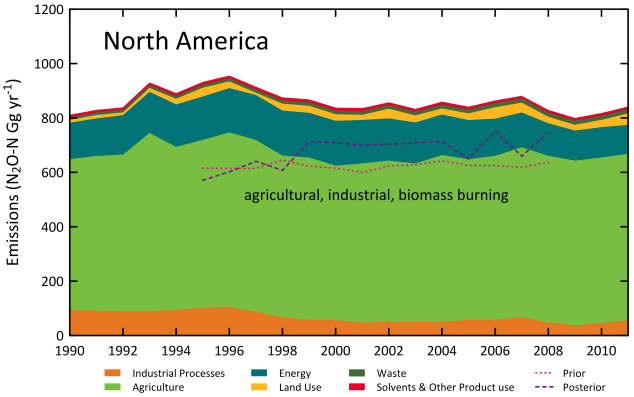

Fig. 5a. Comparison of UNFCCC estimates with our prior (pink dot) and optimized agricultural, industrial, and biomass burning emissions (purple dash) in $GgN_2O\text{-}N\,yr^{-1}$ for North America.

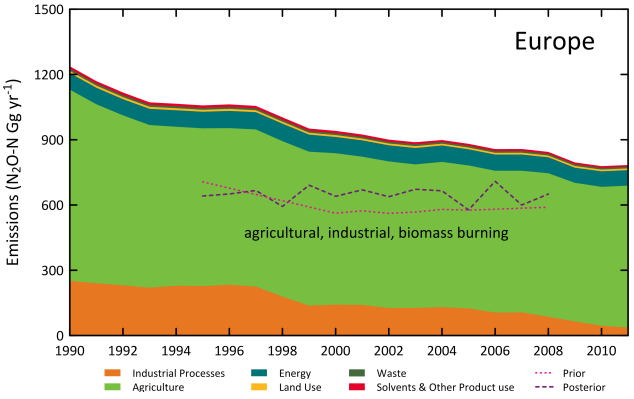

Fig. 5b. Comparison of UNFCCC estimates with our prior (pink dot) and optimized agricultural, industrial, and biomass burning emissions (purple dash) in $GgN_2O\text{-}N\,yr^{-1}$ for Europe.

Asia, and Southern Asia, giving us some confidence in the inversion results. At the same time, we also see some impact of El Niño–Southern Oscillation (ENSO) events on soil emissions. Some of the inter-annual variability we find in soil emissions (see Fig. 3f) is qualitatively correlated with ENSO events. Specifically, decreased emissions are found in El Niño years in Northern Asia, Southern Asia, and North America, whereas the opposite is true for La Niña years. The effect of ENSO on sources and sinks of these emissions is complex (Davidson et al., 2004) and is beyond the scope of this paper. A detailed discussion of ENSO effects on natural soil emissions can be found in Saikawa et al. (2013).

We do not find much inter-annual variability in other sector emissions including industrial and biomass burning. The main reason is because those emissions are smaller, which lead to sensitivities also being equally small. Therefore, we do not obtain a large uncertainty reduction from our inversion as seen in Fig. 3d and h. The only exception where we find a decreased emissions trend is in Southern Asia's biomass burning, where the emissions in recent years are

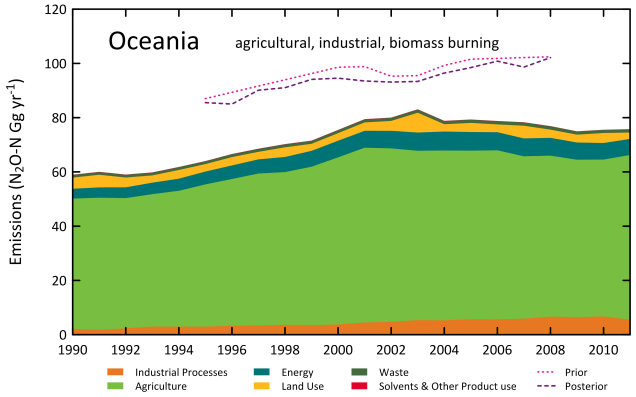

Fig. 5c. Comparison of UNFCCC estimates with our prior (pink dot) and optimized agricultural, industrial, and biomass burning industrial emissions (purple dash) in $GgN_2O\text{-}N\,yr^{-1}$ for Oceania.

much smaller than during the 1990s. However, this is simply due to the prior emissions estimates and is not due to our inversion, as can be seen by the small uncertainty reduction.

4.3 Regional emissions trend

For North America, our mean optimized emissions between 2004 and 2008 are $1.20 \pm 0.20\,TgN_2O\text{-}N\,yr^{-1}$ (Table 4). Here and in all subsequent discussions, the uncertainties we list are one standard deviation. Miller et al. (2012) analyzed tall tower observations in 2004 and 2008 using a Lagrangian model and found peak emissions in June over the central United States. Jeong et al. (2012) have looked at emissions from central California from December 2007 through November 2009, using measurements from a tall tower (Walnut Grove), and they also found posterior emissions to be twice the EDGAR emission inventory estimates. Similarly, Kort et al. (2008), using measurements from the CO_2 Budget and Regional Airborne-North America (COBRA-NA) campaign in May–June 2003 and a Lagrangian model, estimated annual N_2O emissions from North America to be $2.7\,TgN_2O\text{-}N\,yr^{-1}$. As Miller et al. (2012) indicate, extrapolating these values to the US and Canada results in this region accounting for 12–15 % of the total N_2O source and 32–39 % of the global anthropogenic source in 2007. Our estimate suggests that North America is 6.1–8.4 % of the total N_2O source and 20.9–27.0 % of the global anthropogenic source, and they differ from these previous estimates. The discrepancies may be due to these regional inversion results being based on short-term data and from selected sites, whereas our study uses data from six measurement networks with extensive spatial coverage to constrain the global budget. Short-term and regional inversion results might not be appropriate to constrain annual N_2O emissions. At the same time, there is a significant difference in the Lagrangian and Eulerian models that are worth investigating.

However, our estimates agree with other studies conducted in Europe. For example, Corazza et al. (2011) used NOAA/ESRL and other quasi-continuous measurements and a four-dimensional variational (4DVAR) technique with an atmospheric transport zoom model to estimate European emissions in 2006 and quantified annual European N_2O emissions to be 0.78 TgN_2O-N yr^{-1}, and this value is in alignment with ours (0.93 ± 0.12 TgN_2O-N yr^{-1}). Manning et al. (2003) derived annual EU N_2O emissions between 1995 and 2000 using the Numerical Atmospheric Dispersion Modeling Environment (NAME) driven by three-dimensional synoptic meteorology from the Unified Model. Their estimated range, 0.84–0.88 TgN_2O-N yr^{-1}, also agrees with our estimate of 0.83 ± 0.19 TgN_2O-N yr^{-1} for the same period. Our result is also in alignment with Thompson et al. (2011), who used observations from a tower site at Ochsenkopf, Germany and a Lagrangian model to estimate western and central European emissions at a weekly time step in 2007, and found emissions peaked during August and September.

For Asia, Yan et al. (2003), using a bottom-up approach, estimated agricultural emissions from Asian countries (including China, India, Pakistan, Indonesia, Thailand, Philippines, Bangladesh, Myanmar, Viet Nam, Japan, and others) for 1995 to be 1.19 TgN_2O-N yr^{-1}. Our result for agricultural soil from the same region in 1995 is 0.79 ± 0.22 TgN_2O-N yr^{-1}, which is slightly smaller, but this may be due to the difference in the countries included in our estimates.

For North America, Europe, and Oceania, we also compared our posterior emission estimates including agricultural, industrial, and biomass burning emissions using the GMFD forcing data set for natural soil with United Nations Framework Convention on Climate Change (UNFCCC) estimates (United Nations Framework Convention on Climate Change, 2013) (Fig. 5). For North America and Europe, our estimates are lower than the UNFCCC estimates for anthropogenic N_2O emissions. For both of these regions, however, our posterior emission estimates in 2008 are closer to the UNFCCC estimates than in 1995. This is due to our deduced 1995–2008 increase in agricultural soil emissions in North America, and the 1995–2008 decrease in UNFCCC anthropogenic emission estimates in Europe. For Oceania, our estimates are higher than those of UNFCCC, mainly due to our prior estimates being higher than theirs. It is worth noting that there is little uncertainty reduction in Oceania due to the calculated low sensitivities of the measurement sites to emissions from this region (Fig. 3).

We also compared global land and global ocean emissions with the previous estimates. Comparing the global total land budget from our inversions with other previous estimates, we find good agreement. Hirsch et al. (2006) estimated the global total land emissions to be 9.7–13.6 TgN_2O-N yr^{-1} for the period between 1998 and 2001. Our estimate of 12.6 ± 0.59 TgN_2O-N yr^{-1} is in their range. The global ocean emissions estimates vary from as low as 0.90–1.7 TgN_2O-N yr^{-1} (Rhee et al., 2009), 1.2–6.8 TgN_2O-N yr^{-1} (Nevison et al., 1995), 3.8 TgN_2O-N yr^{-1} (Suntharalingam and Sarmiento, 2000), 4.5 TgN_2O-N yr^{-1} (Manizza et al., 2012), 4.5–6.5 TgN_2O-N yr^{-1} (Hirsch et al., 2006), to as high as 5.8–7.8 TgN_2O-N yr^{-1} (Nevison et al., 2003). Our estimates agree with the median value and the average among the 14 years of our calculation is 4.56 ± 0.32 TgN_2O-N yr^{-1}.

The global total that we find from this study is consistent with results from past studies. Our results for the two time periods (1997–2001 and 2002–2005) are 16.8 ± 0.64 and 18.1 ± 0.60 TgN_2O-N yr^{-1}, respectively, and they align with the ranges estimated by Huang et al. (2008) for the same period (15.1–17.8 and 14.1–17.1 TgN_2O-N yr^{-1}, respectively). Our results for 1998–2001 (17.0 ± 0.62 TgN_2O-N yr^{-1}) also compare well with those by Hirsch et al. (2006) (15.2–20.4 TgN_2O-N yr^{-1}). Furthermore, quantifying the ODP-weighted emissions, which provide an estimate of the impact N_2O has on global stratospheric ozone depletion in relative terms, results in 0.47 Mt CFC-11-equivalent in 2008, and this is larger than the sum of the ODS emissions of those controlled by the Montreal Protocol (approximately 0.45 Mt CFC-11-equivalent) (Daniel et al., 2011).

Our results also indicate that the ratio of anthropogenic (including agricultural soil, industrial, and biomass burning) to natural (natural soil and ocean) emissions has increased in recent years in Southern Asia and in Central/South America. In addition to Southern Asia, Central and South America shows a 49 % increase in nitrogen fertilizer consumption between 1995 and 2008 (International Fertilizer Industry Association, 2013). Indeed, the 5 years' mean of the percentage of regional anthropogenic emissions shifts from 69.4 % between 1995 and 1999 to 77.4 % between 2004 and 2008 in Southern Asia, and similarly from 42.6 % to 45.8 % in Central/South America. Our inversion results indicate, however, that the natural soil and ocean emissions still share approximately two-thirds of the global total N_2O emissions, as has been discussed in the past (Werner et al., 2007).

4.4 Inversions using different measurements

In addition to using all measurements, we conducted separate inversions as follows: (1) only including the in situ measurements (AGAGE, NIES, and NOAA RITS & CATS); (2) only including the flask measurements (Surgut aircraft, NOAA CCGG & OTTO, Tohoku University, and CSIRO); and (3) only including AGAGE and NOAA CCGG measurements. We chose these three options because of several reasons. First, by selecting only the in situ and the flask measurements, these comparisons allow us to determine the importance of spatial and temporal resolutions of the measurements in estimating regional emissions by source sector. Second, we excluded measurements that had significant calibration difference to understand how calibration differences could impact the inversion results. For example, AGAGE and NOAA CCGG are on very similar standard scales as shown

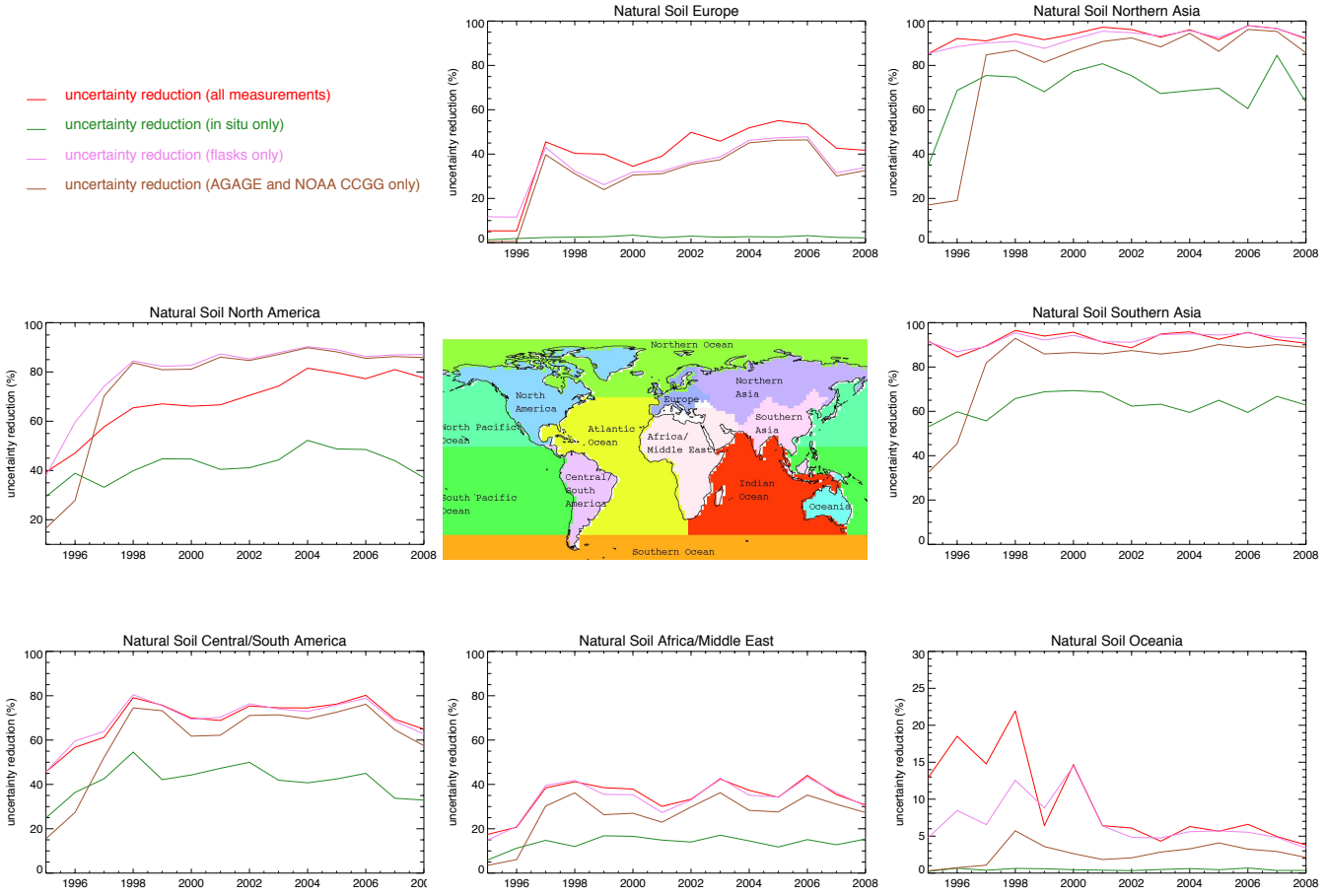

Fig. 6. Comparison of posterior natural soil emissions uncertainty reduction using different sets of measurements. The number of long-time ground measurement sites for each are as follows: all measurements (119), in situ only (12), flasks only (97), and AGAGE and NOAA CCGG only (88)

by frequent comparisons of all measurements, whereas all others have gone through some minor adjustment. Fig. 6 shows the uncertainty reduction for natural soil emissions in seven regions for each inversion.

We find that in all regions except for North America, inversions using all measurements provide the largest uncertainty reduction for natural soil emission estimates most of the time (see Fig. 6). In North America, we achieve the largest uncertainty reductions when including only flask data. The reason the largest uncertainty reduction is not achieved when using all available measurements in this region is due to the differences in measured values at several sites. There are several, such as BRW, MHD, and NWR, where more than three different measurement networks are co-located, and although we do apply ratios to minimize these differences (as explained in Sect. 2), Fig. 6 illustrates that these scale differences still limit our ability to constrain regional emissions. This highlights the need for unification of standard scales and more ongoing measurement comparisons among networks.

In all cases, only including in situ measurements results in the smallest uncertainty reduction due to the spatial sparsity of the data after 1997, when a significant number of NOAA CCGG measurements start. Fig. 6 also illustrates that consistency and wide coverage of the measurements are both very important, especially for analyzing regional emissions by source sector. However, it is important to point out the differences between in situ and flask measurements. In situ measurements are high-frequency measurements that are able to collect a random subset of total N_2O data at a particular site, whereas flask data are for representing the background air at a site. In our coarse-resolution modeling, it is often not possible to make the best use of high-frequency in situ measurements. Such differences between the two measurement networks are especially visible in Europe and Oceania, where the regional coverage is small.

There are several ways we could improve the accuracy of N_2O emissions inferred from inverse modeling in the future. First, expanding measurements in data-sparse regions such as Africa, the Middle East, Eastern Europe, South

Asia, Central/South America, Oceania, Atlantic Ocean, Indian Ocean, and Northern and Southern oceans would allow us to better constrain emissions from these regions, which in turn would also improve the global emission estimate. Second, the use of finer-resolution chemical transport models and meteorology data would also allow us to disaggregate regions further and detect sensitivities to atmospheric mole fractions due to increases in emissions more accurately, as shown by the work of Corazza et al. (2011) focusing on Europe. In the future, we could potentially combine a global Eulerian model with a Lagrangian model to focus on a specific region of interest (Rigby et al., 2011). Third, including the whole stratosphere (e.g., using the Whole Atmosphere Community Climate Model) and better implementation of the stratospheric sink may improve the simulation of stratosphere-troposphere interactions, which could result in a better representation of the monthly variability that we observe in the measurements.

5 Conclusions

We utilized published and new atmospheric mole fraction measurements of N_2O between 1995–2008 from six measurement networks (AGAGE, NOAA CCGG, NOAA OTTO, RITS, and CATS, CSIRO, NIES, and Tohoku University), comprised of archived air samples, flask measurements at a daily, weekly, and monthly frequency (surface, towers, aircrafts, and ships), and high-frequency in situ observations to derive regional emission estimates by source sector. Recently, Thompson et al. (2014) used an extensive network similar to ours for estimating N_2O emissions. Here we included two additional networks in our analysis: NOAA RITS and NOAA OTTO. This is the first time that an almost all-inclusive comprehensive data set has been utilized for an inverse study of N_2O. We estimated regional (seven land and six ocean) emissions of N_2O by source sector (agricultural soil, industrial, natural soil, ocean, and biomass burning) from 1995 to 2008 using these measurements and the global three-dimensional chemical transport model MOZART v4 with a Bayesian inverse methodology. Our estimated emissions generally agree with previously published estimates, although there are major discrepancies in North America between our results and those of Miller et al. (2012), Jeong et al. (2012), and Kort et al. (2008) using a Lagrangian model.

Our regional inversion results indicate no significant emissions increase or reduction in all sectors except in agricultural soil, and we find inter-annual variability in soil emissions. Global total emissions have been increasing in recent years, and we find a significant increasing trend in agricultural soil emissions from Southern Asia, which includes China and India, mostly due to the rise in nitrogen fertilizers in these developing economies, as suggested in the past studies (Davidson, 2009; Park et al., 2012). In addition, we find that the anthropogenic emissions are increasing in Southern Asia and in Central/South America, most likely due to the increase in these agricultural soil emissions.

We do not necessarily obtain the largest uncertainty reduction for our optimized emissions by utilizing all available data. Our inversion results using different combinations of measurements illustrate the importance of unifying measurement scales, as well as broad spatial coverage for regional emissions estimates by source sector. More research is essential to accurately assess regional emissions at a finer scale, especially to investigate the impact of different models used in the study, but we show that soil is the largest source of N_2O emissions and that our optimized N_2O emissions estimate results in ODP-weighted emissions larger than the sum of the ODS emissions of those controlled by the Montreal Protocol.

Supplementary material related to this article is available online at http://www.atmos-chem-phys.net/14/4617/2014/acp-14-4617-2014-supplement.pdf.

Acknowledgements. The AGAGE research program is supported by the NASA Upper Atmospheric Research Program in the US with grants NNX11AF17G to MIT, NNX07AF09G and NNX07AE87G to SIO, Defra/DECC contract GA0201 for support of the Mace Head measurements and NOAA contract RA133R09CN0062 for partial support of Ragged Point in Barbados, CSIRO and the Australian Government Bureau of Meteorology in Australia. For this study MM acknowledges financial support from the post-doctoral fellowship at Scripps Institution of Oceanography and from NASA, grant NNX08AB48G. NOAA provided operational support of the AGAGE systems at American Samoa. We would also like to thank Arlyn Andrews, Nada Derek, David Nance, and Debra Mondeel for their help. NOAA HATS support comes from the NOAA Climate Program Office under their Atmospheric Chemistry, Carbon Cycle, and Climate (AC4) Program. We thank all the staff at the AGAGE, NOAA, CSIRO, NIES, and Tohoku University sites for their contributions to produce high-quality measurements of important atmospheric trace gases. We also thank the two anonymous reviewers for providing constructive comments to the paper.

Edited by: M. Heimann

References

Baker, D. F., Law, R. M., Gurney, K. R., Rayner, P., Peylin, P., Denning, A. S., Bousquet, P., Bruhwiler, L., Chen, Y. H., Ciais, P., Fung, I. Y., Heimann, M., John, J., Maki, T., Maksyutov, S., Masarie, K., Prather, M., Pak, B., Taguchi, S., and Zhu, Z.: TransCom 3 inversion intercomparison: Impact of transport model errors on the interannual variability of regional CO_2 fluxes, 1988–2003, Global Biogeochem. Cy., 20, GB1002, doi:10.1029/2004GB002439, 2006.

Betts, A. K., Zhao, M., Dirmeyer, P. A., and Beljaars, A. C. M.: Comparison of ERA40 and NCEP/DOE near-surface data sets with other ISLSCP-II data sets, J. Geophys. Res., 111, D22S04, doi:10.1029/2006JD007174, doi:10.1029/2006JD007174, 2006.

Bouwman, A. F., Fung, I., Matthews, E., and John, J.: Global analysis of the potential for N_2O production in natural soils, Global Biogeochem. Cy., 7, 557–597, doi:10.1029/93GB01186, 1993.

Chen, Y.-H. and Prinn, R. G.: Estimation of atmospheric methane emissions between 1996 and 2001 using a three-dimensional global chemical transport model, J. Geophys. Res., 111, D10307, doi:10.1029/2005JD006058, 2006.

Corazza, M., Bergamaschi, P., Vermeulen, A. T., Aalto, T., Haszpra, L., Meinhardt, F., O'Doherty, S., Thompson, R., Moncrieff, J., Popa, E., Steinbacher, M., Jordan, A., Dlugokencky, E., Brühl, C., Krol, M., and Dentener, F.: Inverse modelling of European N_2O emissions: assimilating observations from different networks, Atmos. Chem. Phys., 11, 2381–2398, doi:10.5194/acp-11-2381-2011, 2011.

Crutzen, P. J.: The influence of nitrogen oxides on the atmospheric ozone content, Q. J. Roy. Meteorol. Soc., 96, 320–325, doi:10.1002/qj.49709640815, 1970.

Daniel, J. S., Velders, G. J. M., Morgenstern, O., Toohey, D. W., Wallington, T. J., Wuebbles, D. J., Akiyoshi, H., Bais, A. F., Fleming, E. L., Jackman, C. H., Kuijpers, L. J. M., McFarland, M., Montzka, S. A., Ross, M. N., Tilmes, S., Tully, M. B., Andersen, S. O., Langematz, U., and Mingley, P. M.: A Focus on Information on Options for Policymakers, chap. 5, 52, Global Ozone Research and Monitoring Project Report, 2011.

Davidson, E. A.: The contribution of manure and fertilizer nitrogen to atmospheric nitrous oxide since 1860, Nature Geosci., 2, 659–662, doi:10.1038/ngeo608, 2009.

Davidson, E. A., Ishida, F. Y., and Nepstad, D. C.: Effects of an experimental drought on soil emissions of carbon dioxide, methane, nitrous oxide, and nitric oxide in a moist tropical forest, Global Change Biol., 10, 718–730, doi:10.1111/j.1529-8817.200300762.x, 2004.

Denman, K. L., Brasseur, G., Chidthaisong, A., Ciais, P., Cox, P. M., Dickinson, R. E., Hauglustaine, D., Heinze, C., Holland, E., Jacob, D., Lohmann, U., Ramachandran, S., Leite da Silva Dias, P., Wofsy, S. C., and Zhang, X.: Couplings between changes in the climate system and biogeochemistry, chap. 7, Cambridge University Press, Cambridge, UK and New York, NY, USA, 2007.

Dirmeyer, P. A. and Tan, L.: A multi-decadal global land-surface data set of state variables and fluxes, COLA Technical Report 102, Center for Ocean-Land-Atmosphere Studies, Maryland, 2001.

Dlugokencky, E. J., Steele, L. P., Lang, P. M., and Masarie, K. A.: The growth rate and distribution of atmospheric methane, J. Geophys. Res., 99, 17021–17043, doi:10.1029/94JD01245, doi:10.1029/94JD01245, 1994.

Emmons, L. K., Walters, S., Hess, P. G., Lamarque, J.-F., Pfister, G. G., Fillmore, D., Granier, C., Guenther, A., Kinnison, D., Laepple, T., Orlando, J., Tie, X., Tyndall, G., Wiedinmyer, C., Baughcum, S. L., and Kloster, S.: Description and evaluation of the Model for Ozone and Related chemical Tracers, version 4 (MOZART-4), Geosci. Model Dev., 3, 43–67, doi:10.5194/gmd-3-43-2010, 2010.

Engelen, R. J., Denning, A. S., and Gurney, K. R.: On error estimation in atmospheric CO_2 inversions, J. Geophys. Res. Atmos., 107, ACL 10-1–ACL 10-13, doi:10.1029/2002JD002195, doi:10.1029/2002JD002195, 2002.

European Commission, Joint Research Centre (JRC)/Netherlands Environmental Assessment Agency (PBL): Emission Database for Global Atmospheric Research (EDGAR), release version 4.0, http://edgar.jrc.ec.europa.eu (last access: 2 May 2014), 2009.

Firestone, M. K. and Davidson, E. A.: Microbiological basis of NO and N_2O production and consumption in soil, 7–21, John Wiley and Sons, New York, NY, 1989.

Forster, P., Ramaswamy, V., Artaxo, P., Berntsen, T., Betts, R., Fahey, D. W., Haywood, J., Lean, J., Lowe, D. C., Myhre, G., Nganga, J., Prinn, R., Raga, G., Schulz, M., and van Dorland, R.: Changes in Atmospheric Constituents and in Radiative Forcing, chap. 2, Cambridge University Press, United Kingdom and New York, NY, 2007.

Francey, R. J., Steele, L. P., Langenfelds, R. L., Lucarelli, M. P., Allison, C. E., Beardsmore, D. J., Coram, S. A., Derek, N., de Silva, F. R., Etheridge, D. M., Fraser, P. J., Henry, R. J., Turner, B., Welch, E. D., Spencer, D. A., and Cooper, L. N.: Global Atmospheric Sampling Laboratory (GASLAB): supporting and extending the Cape Grim trace gas programs, 8–29, Bureau of Meteorology and CSIRO Division of Atmospheric Research, 1996.

Francey, R. J., Steele, L. P., Spencer, D. A., Langenfelds, R. L., Law, R. M., Krummel, P. B., Fraser, P. J., Etheridge, D. M., Derek, N., Coram, S. A., Cooper, L. N., Allison, C. E., Porter, L., and Baly, S.: The CSIRO (Australia) measurement of greenhouse gases in the global atmosphere, 8–29, World Meteorological Organization Global Atmosphere Watch, 2003.

Groffman, P. M., Hardy, J. P., Driscoll, C. T., and Fahey, T. J.: Snow depth, soil freezing, and fluxes of carbon dioxide, nitrous oxide and methane in a northern hardwood forest, Global Change Biol., 12, 1748–1760, doi:10.1111/j.1365-2486.2006.01194.x, 2006.

Hall, B. D., Dutton, G. S., and Elkins, J. W.: The NOAA nitrous oxide standard scale for atmospheric observations, J. Geophys. Res., 112, D09 305, doi:10.1029/2006JD007954, 2007.

Hirsch, A. I., Michalak, A. M., Bruhwiler, L. M., Peters, W., Dlugokencky, E. J., and Tans, P. P.: Inverse modeling estimates of the global nitrous oxide surface flux from 1998–2001, Global Biogeochem. Cy., 20, doi:10.1029/2004GB002443, 2006.

Holloway, T., Levy, Hiram, I., and Kasibhatla, P.: Global distribution of carbon monoxide, J. Geophys. Res., 105, 12123–12147, doi:10.1029/1999JD901173, 2000.

Hourdin, F., Musat, I., Bony, S., Braconnot, P., Codron, F., Dufresne, J.-L., Fairhead, L., Filiberti, M.-A., Friedlingstein, P., Grandpeix, J.-Y., Krinner, G., LeVan, P., Li, Z.-X., and Lott, F.: The LMDZ4 general circulation model: climate performance and sensitivity to parametrized physics with emphasis on tropical convection, Clim. Dynam., 27, 787–813, doi:10.1007/s00382-006-0158-0, 2006.

Huang, J., Golombek, A., Prinn, R., Weiss, R., Fraser, P., Simmonds, P., Dlugokencky, E. J., Hall, B., Elkins, J., Steele, P., Langenfelds, R., Krummel, P., Dutton, G., and Porter, L.: Estimation of regional emissions of nitrous oxide from 1997 to 2005 using multinetwork measurements, a chemical transport model, and an inverse method, J. Geophys. Res., 113, doi:10.1029/2007JD009381, 2008.

International Fertilizer Industry Association: IFA, http://www.fertilizer.org/ifa/ifadata (last accessed: 26 May 2013), 2013.

Ishijima, K., Nakazawa, T., Sugawara, S., Aoki, S., and Saeki, T.: Concentration variations of tropospheric nitrous oxide over Japan, Geophys. Res. Lett., 28, 171–174, doi:10.1029/2000GL011465, doi:10.1029/2000GL011465, 2001.

Ishijima, K., Nakazawa, T., and Aoki, S.: Variations of atmospheric nitrous oxide concentration in the northern and western Pacific, Tellus B, 61, 408–415, doi:10.1111/j.1600-0889.2008.00406.x, 2009.

Ishijima, K., Patra, P. K., Takigawa, M., Machida, T., Matsueda, H., Sawa, Y., Steele, L. P., Krummel, P. B., Langenfelds, R. L., Aoki, S., and Nakazawa, T.: Stratospheric influence on the seasonal cycle of nitrous oxide in the troposphere as deduced from aircraft observations and model simulations, J. Geophys. Res., 115, D20308, doi:10.1029/2009JD013322, 2010.

Jeong, S., Zhao, C., Andrews, A. E., Dlugokencky, E. J., Sweeney, C., Bianco, L., Wilczak, J. M., and Fischer, M. L.: Seasonal variations in N_2O emissions from central California, Geophys. Res. Lett., 39, L16 805, doi:10.1029/2012GL052307, 2012.

Kaminski, T., Rayner, P. J., Heimann, M., and Enting, I. G.: On aggregation errors in atmospheric transport inversions, J. Geophys. Res. Atmos., 106, 4703–4715, doi:10.1029/2000JD900581, 2001.

Khalil, M. A. K., Rasmussen, R. A., and Shearer, M. J.: Atmospheric nitrous oxide: patterns of global change during recent decades and centuries, Chemosphere, 47, 807–821, doi:10.1016/S0045-6535(01)00297-1, 2002.

Kort, E. A., Eluszkiewicz, J., Stephens, B. B., Miller, J. B., Gerbig, C., Nehrkorn, T., Daube, B. C., Kaplan, J. O., Houweling, S., and Wofsy, S. C.: Emissions of CH_4 and N_2O over the United States and Canada based on a receptor-oriented modeling framework and COBRA-NA atmospheric observations, Geophys. Res. Lett., 35, L18808, doi:10.1029/2008GL034031, doi:10.1029/2008GL034031, 2008.

Kort, E. A., Patra, P. K., Ishijima, K., Daube, B. C., Jimenez, R., Elkins, J., Hurst, D., Moore, F. L., Sweeney, C., and Wofsy, S. C.: Tropopsheric distribution and variability of N_2O: Evidence for strong tropical emissions, Geophys. Res. Lett., 38, L15806, doi:10.1029/2011GL047612, 2011.

Kreileman, G. J. J. and Bouwman, A. F.: Computing land use emissions of greenhouse gases, Water Air Soil Pollut., 76, 231–258, doi:10.1007/BF00478341, 1994.

Li, C., Frolking, S., and Frolking, T. A.: A Model of Nitrous Oxide Evolution From Soil Driven by Rainfall Events: 1. Model Structure and Sensitivity, J. Geophys. Res., 97, 9759–9776, 1992.

Manizza, M., Keeling, R. F., and Nevison, C. D.: On the processes controlling the seasonal cycles of the air-sea fluxes of O_2 and N_2O: A modelling study, Tellus B, 64, 14829, doi:10.3402/tellusb.v64i0.18429, 2012.

Manning, A. J., Ryall, D. B., Derwent, R. G., Simmonds, P. G., and O'Doherty, S.: Estimating European emissions of ozone-depleting and greenhouse gases using observations and a modeling back-attribution technique, J. Geophys. Res. Atmos., 108, 4405, doi:10.1029/2002JD002312, 2003.

Meirink, J. F., Bergamaschi, P., and Krol, M. C.: Four-dimensional variational data assimilation for inverse modelling of atmospheric methane emissions: method and comparison with synthesis inversion, Atmos. Chem. Phys., 8, 6341–6353, doi:10.5194/acp-8-6341-2008, 2008.

Miller, S. M., Kort, E. A., Hirsch, A. I., Dlugokencky, E. J., Andrews, A. E., Xu, X., Tian, H., Nehrkorn, T., Eluszkiewicz, J., Michalak, A. M., and Wofsy, S. C.: Regional sources of nitrous oxide over the United States: Seasonal variation and spatial distribution, J. Geophys. Res., 117, D06310, doi:10.1029/2011JD016951, 2012.

Minschwaner, K., Salawitch, R. J., and McElroy, M. B.: Absorption of solar radiation by O_2: Implications for O_3 and lifetimes of N_2O, $CFCl_3$, and CF_2Cl_2, J. Geophys. Res. Atmos., 98, 10543–10561, doi:10.1029/93JD00223, 1993.

Montzka, S. A., Reimann, S., Engel, A., Krüger, K., O'Doherty, S., Sturges, W. T., Blake, D., Dorf, M., Fraser, P., Froidevaux, L., Jucks, K., Kreher, K., Kurylo, M. J., Mellouki, A., Miller, J., Nielsen, O.-J., Orkin, V. L., Prinn, R. G., Rhew, R., Santee, M. L., Stohl, A., and Verdonik, D.: Ozone-Depleting Substances (ODSs) and Related Chemicals, chap. 1, 52, p. 516, Global Ozone Research and Monitoring Project – Report, Geneva, Switzerland, 2011.

Nevison, C., Butler, J. H., and Elkins, J. W.: Global distribution of N_2O and the ΔN_2O-AOU yield in the subsurface ocean, Global Biogeochem. Cy., 17, 1119, doi:10.1029/2003GB002068, 2003.

Nevison, C. D., Weiss, R. F., and Erickson, D. J.: Global oceanic emissions of nitrous oxide, J. Geophys. Res., 100, 15809–15820, 1995.

Nevison, C. D., Mahowald, N. M., Weiss, R. F., and Prinn, R. G.: Interannual and seasonal variability in atmospheric N_2O, Global Biogeochem. Cy., 21, GB3017, doi:10.1029/2006GB002755, 2007.

Ngo-Duc, T., Polcher, J., and Laval, K.: A 53-year forcing data set for land surface models, J. Geophys. Res., 110, D06116, doi:10.1029/2004JD005434, 2005.

Park, S., Croteau, P., Boering, K. A., Etheridge, D. M., Ferretti, D., Fraser, P. J., Kim, K.-R., Krummel, P. B., Langenfelds, R. L., van Ommen, T. D., Steele, L. P., and Trudinger, C. M.: Trends and seasonal cycles in the isotopic composition of nitrous oxide since 1940, Nature Geosci., 5, 261–265, doi:10.1038/ngeo1421, 2012.

Potter, C. S., Randerson, J. T., Field, C. B., Matson, P. A., Vitousek, P. M., Mooney, H. A., and Klooster, S. A.: Terrestrial ecosystem production: A process model based on global satellite and surface data, Global Biogeochem. Cy., 7, 811–841, doi:10.1029/93GB02725, 1993.

Potter, C. S., Matson, P. A., Vitousek, P. M., and Davidson, E. A.: Process modeling of controls on nitrogen trace gas emissions from soils worldwide, J. Geophys. Res., 101, 1361–1377, 1996.

Prather, M. J., Holmes, C. D., and Hsu, J.: Reactive greenhouse gas scenarios: Systematic exploration of uncertainties and the role of atmospheric chemistry, Geophys. Res. Lett., 39, L09803, doi:10.1029/2012GL051440, 2012.

Prinn, R. G.: Measurement equation for trace chemicals in fluids and solution of its inverse, in: Inverse Methods in Global Biogeochem. Cy., edited by: Kashibhatla, P., Heimann, M., Rayner, P., Mahowald, N., Prinn, R. G., and Hartley, D. E., vol. 114 of Geophys. Monogr. Ser., 3–18, AGU, 2000.

Prinn, R. G., Cunnold, D., Rasmussen, R., Simmonds, P., Alyea, F., Crawford, A., Fraser, P., and Rosen, R.: Atmospheric Emissions and Trends of Nitrous Oxide Deduced From 10 Years of ALE-GAGE Data, J. Geophys. Res., 95, 18369–18385, 1990.

Prinn, R. G., Weiss, R. F., Fraser, P. J., Simmonds, P. G., Cunnold, D. M., Alyea, F. N., O'Doherty, S., Salameh, P., Miller, B. R., Huang, J., Wang, R. H. J., Hartley, D. E., Harth, C., Steele, L. P., Sturrock, G., Midgley, P. M., and McCulloch, A.: A history of chemically and radiatively important gases in air deduced from ALE/GAGE/AGAGE, J. Geophys. Res., 105, 17751–17792, doi:10.1029/2000JD900141, 2000.

Qian, T., Dai, A., Trenberth, K. E., and Oleson, K. W.: Simulation of Global Land Surface Conditions from 1948 to 2004. Part I: Forcing Data and Evaluations, J. Hydrometeorol., 7, 953–975, doi:10.1175/JHM540.1, 2006.

Randerson, J. T., Hoffman, F. M., Thornton, P. E., Mahowald, N. M., Lindsay, K., Lee, Y. H., Nevison, C. D., Doney, S. C., Bonan, G., Stockli, R., Covey, C., Running, S. W., and Fung, I. Y.: Systematic Assessment of Terrestrial Biogeochemistry in Coupled Climate-Carbon Models, Global Change Biol., 15, 2462–2484, 2009.

Rasch, P. J., Mahowald, N. M., and Eaton, B. E.: Representations of transport, convection, and the hydrologic cycle in chemical transport models: Implications for the modeling of short-lived and soluble species, J. Geophys. Res., 102, 28127–28138, doi:10.1029/97JD02087, 1997.

Ravishankara, A. R., Daniel, J. S., and Portmann, R. W.: Nitrous Oxide (N_2O): The Dominant Ozone-Depleting Substance Emitted in the 21st Century, Science, 326, 123–125, 2009.

Rhee, T. S., Kettle, A. J., and Andreae, M. O.: Methane and nitrous oxide emissions from the ocean: A reassessment using basin-wide observations in the Atlantic, J. Geophys. Res. Atmos., 114, D12304, doi:10.1029/2008JD011662, 2009.

Rienecker, M. M., Suarez, M. J., Gelaro, R., Todling, R., Bacmeister, J., Liu, E., Bosilovich, M. G., Schubert, S. D., Takacs, L., Kim, G.-K., Bloom, S., Chen, J., Collins, D., Conaty, A., da Silva, A., Gu, W., Joiner, J., Koster, R. D., Lucchesi, R., Molod, A., Owens, T., Pawson, S., Pegion, P., Redder, C. R., Reichle, R., Robertson, F. R., Ruddick, A. G., Sienkiewicz, M., and Woollen, J.: MERRA: NASA's Modern-Era Retrospective Analysis for Research and Applications, Journal of Climate, 24, 3624–3648, doi:10.1175/JCLI-D-11-00015.1, doi:10.1175/JCLI-D-11-00015.1, 2011.

Rigby, M., Mühle, J., Miller, B. R., Prinn, R. G., Krummel, P. B., Steele, L. P., Fraser, P. J., Salameh, P. K., Harth, C. M., Weiss, R. F., Greally, B. R., O'Doherty, S., Simmonds, P. G., Vollmer, M. K., Reimann, S., Kim, J., Kim, K. R., Wang, H. J., Dlugokencky, E. J., Dutton, G. S., Hall, B. D., and Elkins, J. W.: History of atmospheric SF_6 from 1973 to 2008, Atmos. Chem. Phys., 10, 10305–10320, doi:10.5194/acp-10-10305-2010, 2010.

Rigby, M., Manning, A. J., and Prinn, R. G.: Inversion of long-lived trace gas emissions using combined Eulerian and Lagrangian chemical transport models, Atmos. Chem. Phys., 11, 9887–9898, doi:10.5194/acp-11-9887-2011, 2011.

Saikawa, E., Rigby, M., Prinn, R. G., Montzka, S. A., Miller, B. R., Kuijpers, L. J. M., Fraser, P. J. B., Vollmer, M. K., Saito, T., Yokouchi, Y., Harth, C. M., Mühle, J., Weiss, R. F., Salameh, P. K., Kim, J., Li, S., Park, S., Kim, K.-R., Young, D., O'Doherty, S., Simmonds, P. G., McCulloch, A., Krummel, P. B., Steele, L. P., Lunder, C., Hermansen, O., Maione, M., Arduini, J., Yao, B., Zhou, L. X., Wang, H. J., Elkins, J. W., and Hall, B.: Global and regional emissions estimates for HCFC-22, Atmos. Chem. Phys., 12, 10033–10050, doi:10.5194/acp-12-10033-2012, 2012.

Saikawa, E., Schlosser, C. A., and Prinn, R. G.: Global modeling of soil nitrous oxide emissions from natural processes, Global Biogeochem. Cy., 27, 972–989, doi:10.1002/gbc.20087, 2013.

Sheffield, J., Goteti, G., and Wood, E. F.: Development of a 50-Year High-Resolution Global Dataset of Meteorological Forcings for Land Surface Modeling, J. Climate, 19, 3088–3111, 2006.

Suntharalingam, P. and Sarmiento, J. L.: Factors governing the oceanic nitrous oxide distribution: Simulations with an ocean general circulation model, Global Biogeochem. Cy., 14, 429–454, doi:10.1029/1999GB900032, 2000.

Thompson, R. L., Gerbig, C., and Rödenbeck, C.: A Bayesian inversion estimate of N_2O emissions for western and central Europe and the assessment of aggregation errors, Atmos. Chem. Phys., 11, 3443–3458, doi:10.5194/acp-11-3443-2011, 2011.

Thompson, R. L., Chevallier, F., Crotwell, A. M., Dutton, G., Langenfelds, R. L., Prinn, R. G., Weiss, R. F., Tohjima, Y., Nakazawa, T., Krummel, P. B., Steele, L. P., Fraser, P., O'Doherty, S., Ishijima, K., and Aoki, S.: Nitrous oxide emissions 1999 to 2009 from a global atmospheric inversion, Atmos. Chem. Phys., 14, 1801–1817, doi:10.5194/acp-14-1801-2014, 2014. 2013.

Thompson, R. L., Patra, P. K., Ishijima, K., Saikawa, E., Corazza, M., Karstens, U., Wilson, C., Bergamaschi, P., Dlugokencky, E., Sweeney, C., Prinn, R. G., Weiss, R. F., O'Doherty, S., Fraser, P. J., Steele, L. P., Krummel, P. B., Saunois, M., Chipperfield, M., and Bousquet, P.: TransCom N_2O model inter-comparison – Part 1: Assessing the influence of transport and surface fluxes on tropospheric N_2O variability, Atmos. Chem. Phys., 14, 4349–4368, doi:10.5194/acp-14-4349-2014, 2014.

Thornton, P. E., Lamarque, J. F., Rosenbloom, N. A., and Mahowald, N. M.: Influence of carbon-nitrogen cycle coupling on land model response to CO_2 fertilization and climate variability, Global Biogeochem. Cy., 21, GB4018, doi:10.1029/2006GB002868, 2007.

Thornton, P. E., Doney, S. C., Lindsay, K., Moore, J. K., Mahowald, N., Randerson, J. T., Fung, I., Lamarque, J.-F., Feddema, J. J., and Lee, Y.-H.: Carbon-nitrogen interactions regulate climate-carbon cycle feedbacks: results from an atmosphere-ocean general circulation model, Biogeosciences, 6, 2099–2120, doi:10.5194/bg-6-2099-2009, 2009.

Tohjima, Y., Mukai, H., Maksyutov, S., Takahashi, Y., Machida, T., Katsumoto, M., and Fujinuma, Y.: Variations in atmospheric nitrous oxide observed at Hateruma monitoring station, Chemosphere – Global Change Sci., 2, 435–443, 2000.

United Nations Framework Convention on Climate Change: National Inventory Submissions 2013, http://unfccc.int/national_reports/annex_i_ghg_inventories/national_inventories_submissions/items/7383.php (last access: 22 October 2013), 2013.

van der Werf, G. R., Randerson, J. T., Giglio, L., Collatz, G. J., Mu, M., Kasibhatla, P. S., Morton, D. C., DeFries, R. S., Jin, Y., and van Leeuwen, T. T.: Global fire emissions and the contribution of deforestation, savanna, forest, agricultural, and peat fires (1997–2009), Atmos. Chem. Phys., 10, 11707–11735, doi:10.5194/acp-10-11707-2010, 2010.

van Noije, T. P. C., Eskes, H. J., van Weele, M., and van Velthoven, P. F. J.: Implications of the enhanced Brewer-Dobson circulation in European Centre for Medium-Range Weather Forecasts reanalysis ERA-40 for the stratosphere-troposphere exchange of ozone in global chemistry transport models, J. Geophys. Res., 109, D19308, doi:10.1029/2004JD004586, doi:10.1029/2004JD004586, 2004.

Werner, C., Kiese, R., and Butterbach-Bahl, K.: Soil-atmosphere exchange of N_2O, CH_4, and CO_2 and controlling environmental factors for tropical rain forest sites in western Kenya, J. Geophys. Res., 112, D03308, doi:10.1029/2006JD007388, 2007.

Xiao, X., Prinn, R. G., Fraser, P. J., Weiss, R. F., Simmonds, P. G., O'Doherty, S., Miller, B. R., Salameh, P. K., Harth, C. M., Krummel, P. B., Golombek, A., Porter, L. W., Butler, J. H., Elkins, J. W., Dutton, G. S., Hall, B. D., Steele, L. P., Wang, R. H. J., and Cunnold, D. M.: Atmospheric three-dimensional inverse modeling of regional industrial emissions and global oceanic uptake of carbon tetrachloride, Atmos. Chem. Phys., 10, 10421–10434, doi:10.5194/acp-10-10421-2010, 2010.

Yan, X., Akimoto, H., and Ohara, T.: Estimation of nitrous oxide, nitric oxide and ammonia emissions from croplands in East, Southeast and South Asia, Global Change Biol., 9, 1080–1096, doi:10.1046/j.1365-2486.2003.00649.x, 2003.